Marlies Christina Hölzl, BSc

Identification and characterisation of neuroendocrine cancer stem cells in P-STS cell line

MASTERARBEIT

zur Erlangung des akademischen Grades

Master of Science

Masterstudium Biochemie und Molekulare Biomedizin

eingereicht an der

Technischen Universität Graz

Betreuerin

ao.Univ.Prof.in i.R. Dr.in phil. Roswitha Pfragner

Univ.-Ass.in Mag.a Dr.in Nassim Ghaffari Tabrizi-Wizsy

Pathophysiology and Immunology Medical University Graz

Graz, Oktober 2014

EIDESSTATTLICHE ERKLÄRUNG

Ich erkläre an Eides statt, dass ich die vorliegende Arbeit selbstständig verfasst, andere als die angegebenen Quellen/Hilfsmittel nicht benutzt, und die den benutzten Quellen wörtlich und inhaltlich entnommenen Stellen als solche kenntlich gemacht habe. Das in TUGRAZonline hochgeladene Textdokument ist mit der vorliegenden Masterarbeit identisch.

I declare that I have authored this thesis independently, that I have not used other

than the declared sources/resources, and that I have explicitly indicated all material which has been quoted either literally or by content from the

Datum / Date

Unterschrift / Signature

ACKNOWLEDGEMENTS

It would not have been possible to write this master thesis without the help and support of the kind people around me, to only some of whom it is possible to give particular mention here.

First of all, I would like to express my sincere thanks to Dr. Nassim Ghaffari Tabrizi-Wizsy for giving me the opportunity to do my master thesis within her group. This gave me the possibility of entering the exciting scientific fields of cancer research. I also want to thank Prof. Roswitha Pfragner for supporting me by fruitful discussion and providing the cell lines. I would also like to thank the company SFL for their special financial support. Thanks to my colleagues and friends, Christina Passegger and Corinna Krump, for their help, support and reception. It was always a pleasure to work with you two! A big thank you to all the members of the Institute of Pathophysiology and Immunology for a pleasant working environment, for all the nice talks and for convivial lunchtime, I always felt like a family member.

My sincere thanks go to all my friends, especially Nikolaus Turrini, who was always willing to lend me his ears, help, or simply be there for me. I am very grateful for your friendship.

And last but not least, I would like to thank my family for their support and great patience at all time. I want to thank my husband, Stefan, for his fundamental belief in my abilities. A special thanks to my parents, Alfons and Barbara, for their never-ending encouragement, ongoing support and giving me enough energy to keep going. Thanks to my beloved older brother, Stefan, who manage to relieve my mind with his peaceful nature and always was there for me whenever I needed him.
I cannot imagine what I would have done without my family.
I love you all so, so much!

THANK YOU!!!

CONTENT

LIST OF FIGURES

LIST OF TABLES

ABBREVIATIONS

5-HT	5-Hydroxytryptamin
ABCG 2	ATP-binding cassette transporter
ALHD	Aldehyde dehydrogenase
bHLH	Basic helix-turn-helix
BMI-1	Polycomb-complex-protein
CAM	Chorioallantoic membrane
CSC	Cancer stem cell
CT	Computer tomography
DEAB	Diethylaminobenzaldehyde
FBS	Fetal bovine serum
GI	Gastrointestinal
HLH	Helix-turn-helix
ID-1	Inhibitor of DNA binding 1
IHC	Immunohistochemistry
MEN1	Multiple endocrine neoplasia type 1
MEN2	Multiple endocrine neoplasia type 2
MSI-1	Musashi-1
NCI	National Cancer Institute's
NEC	neuroendocrine carcinomas
NET	Neuroendocrine tumour
NF1	Neurofibromastosis
NTC	Non transcribed control
Oct-4	Octamer-binding transcription 4
P/S	Penecilin/Streptomycin
PDPN	Podoplanin
PET	Positron emission tomography
PFA	Paraformaldehyde
qPCR	Quantitative PCR
RT	Reverse transcription
SEER	Surveillance, Epidemiology and End Results
Sox-2	Sex-determining region Y-box 2
TF	Transcription factors

ABSTRACT

Background: Neuroendocrine tumours (NETs) represent a group of relatively rare neoplasms derived from the diffuse neuroendocrine system with the propensity to secrete a variety of peptide hormones and biogenic amines. Tumours of these cells are characterized by a relatively indolent rate of growth and appearance of metastasis at the time of diagnosis. In the last years incidence of NETs has risen and response rates to standard chemotherapy and radiotherapy are low.

Cancer stem cells (CSCs) are defined as a small subpopulation, 1-5% of the tumour bulk, which might be responsible for growth and tumourigenesis. CSCs are capable of self-renewal, force tumour invasion and cell differentiation. The presence of CSC is proven in different tumours and might be a new attempt of more promising cancer drugs.

Aims: The aim of this study was to characterize cancer stem cells in P-STS – a well-established gastrointestinal NET cell line – and isolate and improve the impact of these cells on tumourigenesis.

Methods: The P-STS cell line, established from a small intestine metastatic human carcinoid of a 42-year-old male, was used to investigate 4 CSC related surface markers as well as expression of 14 CSC related genes. Furthermore an Aldehyde dehydrogenase activity (ALDH)assay and a spheroid-forming assay were performed. The invasive capacity of 2D *vs.* 3D cells was analysed by chicken chorioallantoic membrane (CAM) assay.

Results: The P-STS cell line revealed an $ALDH^+$ subpopulation as well as a high expression of the investigated CD markers. The ability to form spheroids was proofed. The investigated CSC related genes are expressed in P-STS cell line, even though their expression is significantly higher in 3D spheroids than in the 2D monolayer. The CAM assay proved a more invasive behaviour of spheroids *in vivo* in relation to monolayer cultured cells.

Conclusion: In conclusion, I provided the evidence that P-STS cell line exhibit various characteristics of a CSC subpopulation. P-STS cells express CSC specific genes, which are up-regulated in spheroids. Furthermore, the invasion rate is decreased due to 3D cultivation. My finding may pave the way towards more efficient treatment of therapy resistant NETs.

ZUSAMMENFASSUNG

Hintergrund: Neuroendokrine Tumore (NETs) gehören zu einer Gruppe von relativ seltenen Neoplasmen, die aus dem diffusen Neuroendokrinen System stammen und dazu neigen, verschiedenste Peptide und biogene Amine abzusondern. Charakteristisch für Zellen dieser Tumore ist ein träges Wachstum und Metastasen, die meistens zum Zeitpunkt der Diagnose bereits vorhanden sind. Die Ansprechrate auf Standard-Therapeutika und Strahlentherapie ist sehr gering; zusätzlich kam es in den letzten Jahren zu einer Zunahme der Inzidenz von NETs.

Krebs-Stammzellen, die vermutlich verantwortlich für Wachstum und Tumorgenese sind, machen einen geringen Anteil der Tumormasse aus (1-5%). Die Krebs-Stammzellen konnten in diversen Tumoren nachgewiesen werden und sind im Stande sich selbst zu erneuern, sowie Zellinvasion und Differenzierung zu begünstigen. Des Weiteren erweisen sich Krebs-Stammzellen als sehr vielversprechend hinsichtlich der Entwicklung neuer Krebstherapeutika.

Methoden: Die P-STS Zelllinie wurde in meiner Arbeit zunächst auf die Expression von Stammzellspezifischen Markern untersucht. Zusätzlich wurde eine Aldehyd-Dehyrogenase (ALDH) Aktivität und die Bildung von Tumor-Spheroiden getestet. Das invasive Verhalten der Zellen, die in konventionellen 2D Kulturen gehalten werden im Vergleich mit Zellen, die in 3D Spheroiden wachsen, wurde *via* Chorion Allantois-Membran Assay des Hühnerembryos (CAM Assay) überprüft.

Resultate: Die P-STS Zelllinie weist sowohl eine $ALDH^+$ Subpopulation als auch eine Expression der ermittelten CD-Marker auf. Durch die erfolgreiche Herstellung von 3D Spheroiden, wurde die Expression von Krebs-Stammzellen signifikant erhöht.. Darüber hinaus wurde ein invasiveres Verhalten der 3D Kultivierung auf dem CAM Assay festzustellen.

Schlussfolgerung: Ich konnte zeigen, dass die P-STS Zellen verschiedenste Charakteristika einer Krebs-Stammzellen-Subpopulation aufweisen, sie exprimieren Stammzellmarker, die in Spheroiden hochreguliert werden und die Invasionsrate steigt ebenso, wenn die Zellen 3D kultiviert werden. Diese Erkenntnisse, könnten neue Wege für eine gezielte Behandlung dieser therapieresistenten Tumore eröffnen.

1. INTRODUCTION

1.1. Neuroendocrine tumours

Neuroendocrine tumours (NETs) represent a group of relatively rare neoplasms derived from the diffuse neuroendocrine system. The neuroendocrine system consists of cells, single or arranged in small groups, which are distributed all over various tissues and organs (Figure 1).[1] The term *neuroendocrine* describes 2 properties of these cells: *neuron* because of its neural origin and *endocrine* due to the hormone producing function. These cells generate peptide hormones and biogenic amines and store them in vesicles. Secretion is induced by chemical and mechanical signals and is regulated by G-protein-coupled receptor ion-gated receptors and receptors with tyrosine kinase activity.[2]

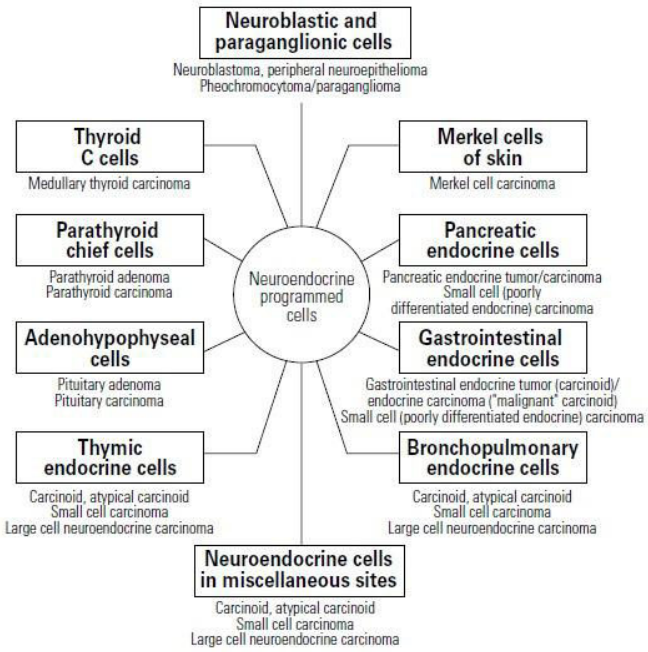

Figure 1 Spectrum of neuroendocrine cells and associated tumours[1]

The US National Cancer Institute's (NCI) Surveillance, Epidemiology and End Results (SEER) database reported an incidence rate of NETs from 1.09 to 5.25/10000 enhanced prevalence over the last forty years. The Swedish national's database published quite similar results of incidence rates.[3] Thus, reasons for the increase of disease reflect the development of better diagnostic tools like

radiological imaging. By analyzing the family risk seems to be the only identified risk factor.[2, 3] The overall 5-year survival of patients with small intestinal NETs (60%), this percentage has not changed since 1973. This remains a disappointing fact and request further investigation. Therefore development of improved methods for early diagnosis, discovering of new therapeutics and performing a more effective management of the disease are required.[4]

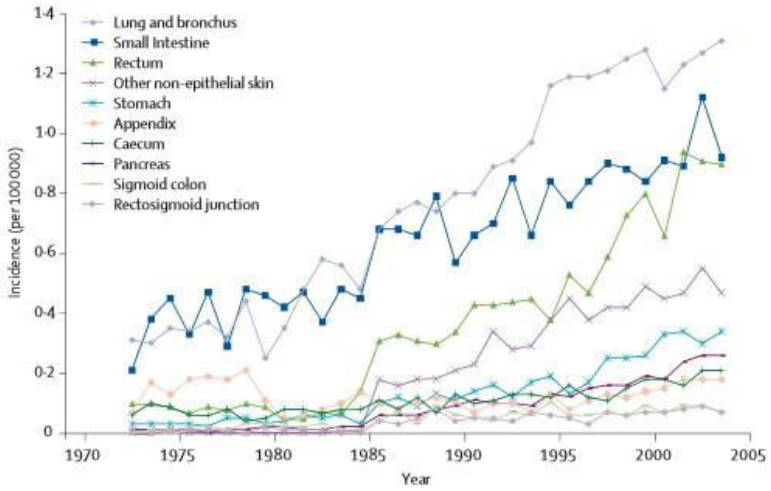

Figure 2 Increased incidence of carcinoid tumours, US population 1973–2005. Overall increase recorded for all primary sites during this period. Data from SEER database, US National Cancer Institute.[2, 3]

NETs are induced sporadically, however some genetic syndromes, multiple endocrine neoplasia type 1 and 2 (MEN1; MEN2), neurofibromastosis (NF1) or Hippel-Lindau disease, can enhance the risk of tumour development. The detection of the tumour depends on the location of the primary tumour and whether it is a so called functional or non-functional tumour. In contrast to non-functional NETs, the functional NETs overproduce hormones, a variety of peptide hormones and biogenic amines, which frequently cause various clinical syndromes, furthermore these tumours are characterised by a relatively indolent rate of growth.[2, 5] NETs are characterised and detected by various methods, inter alia histological markers such as chromogranin-A, synaptophysin and neuron-specific enolase in combination with the presence of secretory granules.[6]

A general marker for NET tumour detection is the testing of Plasma chromogranin-A. In addition to this biochemical testing could be compared with markers related to the location of the tumour, e.g. foregut: Chromogranin-A, chromogranan-B, grastrin, somatostatin, urine histamine metabolites and urine cortisol and so on. To

localise the NET tumour a standard radiological investigation is an abdominal ultrasonography. With the help of this method it is possible to find liver metastasis or primary tumours, which are verified via ultrasound-guided coarse needle biopsy. A computed tomography (CT), magnetic resonance imaging (MRI) or positron emission tomography (PET) is not only used for the localisation, it is also used to choose the right treatment.[7]

Approximately 60% of all NETs are found in the gastrointestinal (GI) tract. In the 19th century GI-NETs were described for the first time by Lubarsch and Ransom, but the closer characterisation failed. Eventually, in 1907 Siegfried Oberndorfer introduced the term "carcinoid" for the NETs of midgut.[2, 8] Because of the historical occurrences a standardized nomenclature is still difficult. Especially the rareness of the tumours and the appearance in different cell types, are reasons why the establishment of a general classification for NETs did not work out in the past.[9] The determination foregut, midgut and hindgut for GI-NETs is based on pathological appearance and was submitted by Williams and Sandler in 1963.[10] Unfortunately this nomenclature system was not correlated with the clinical behaviour and prognosis. In the year 2000 the WHO published a classification schema (shown in **Table 1**) based on Capella *et al*. who divided the NET's into "well differentiated NET's" and "neuroendocrine carcinomas (NECs)".[9]

Table 1 Classification of gastric NETs (WHO 2000)[9]

1. **. Well differentiated NET (synonym: carcinoid)**
   - Benign: =1 cm in size, confined to mucosa-submucosa, no angioinvasion.
   - Uncertain malignant potential (benign or low grade malignant): = 2 cm in size, confined to mucosa-submucosa, with or without angioinvasion.
2. **Well differentiated NEC (synonym: malignant carcinoid)**
   - Low grade malignant: >2 cm in size, invading muscularis propria and beyond, or metastases.
3. **Poorly differentiated NEC**
   - High grade malignant

GI-NETs arise throughout the whole length of the gut. So far, 13 neuroendocrine cell types are identified in the gut, which belong to the most hormone-producing

cells in the body. The majority of GI-NETs are non-functional, with late onset of symptoms, and often have developed metastasis at the time of detection.[2]
The clinical features of GI-NETS are unspecific and similar to common other unspecific diseases. Common symptoms are weight loss, nausea, vomiting, anaemia and abdominal pain. The symptoms from functional NETs are rather cutaneous flushing, diarrhoea and bronchospasm.[11]

1.2. Cancer stem cell theory

Tumour comprises a small subpopulation, 1-5% of the tumour bulk, which might be responsible for growth and tumourigenesis. This cell subpopulation is called cancer stem cells (CSC), named after normal stem cells because of their similar properties. Normal stem cells as well as CSCs are capable of initiate self-renewal, where one cell produces an identical daughter cell, and a more differentiated cell, which is able to generate the vast majority of tumour bulk.[12] In the last thirty years several lines of evidence strengthen the existence of CSCs:
Even though Bruce *et al.* in 1963 mentioned that only a small population (1-4%) of lymphoma cells were responsible for tumour initiation in mice spleen, cancer was seen as a homogeneous mass of proliferating cells with identical alterations.[13] The first evidence of cancer stem cells was published in 1997 by Bonnet and Dick. Their results exposed a $CD34^+/CD38^-$ population of human acute myeloid leukemia (AML) cells with the ability of self-renewal, proliferation and differentiation.[14] Al-Hajj *et al.* identified and isolated CSCs from breast cancer using CD44 and CD24 surface markers.[15] Since that time, CSCs have been discovered in a variety of malignant tumours, such as glioblastoma [16], melanoma [17], osteosarcoma and chondrosarcoma[18], prostate cancer[19], ovarian cancer [20], bladder cancer [21], colorectal cancer [22] and lung cancer[23]. The list keeps getting longer.

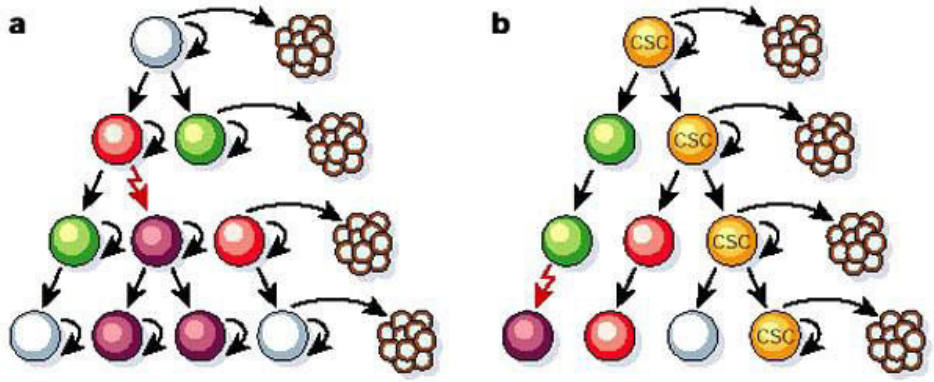

Figure 3 Two controversial models of tumour growth and maintenance. a: stochastic model - every cell of the tumour bulk has the potential to differentiate; b: CSC model - only a small specific subpopulation, CSCs, has the ability to differentiate to induce tumour growth. [24]

These days two controversial models try to explain the cancer development:
The "traditional" stochastic model claims that every cell in a tumour bulk has the same potential to initiate differentiation and proliferation. The heterogeneity originates from a combination of extrinsic- and intrinsic factors, which can control the unique behaviour of each cell. Thus, the cell is governed by their surrounding environment and signals; tumour cells are unpredictable and follow no hierarchical system.[24, 25]

The second model, however, follows a hierarchical system where each cell has a different growth capacity. The largest component constitutes "normal" tumour cells, which are non-proliferative and have to be replaced by new ones. Progenitor cells are highly proliferative and responsible to replenish the whole tumour bulk cells, but lack of self-renewal. On the apex of the hierarchy are the cancer stem cells. This small population is capable of self-renewal as well as responsible to retreat tumour heterogeneity by generating identical daughter and progenitor cells.[25]

Even though these two models aspire different approaches, none of them can be declined. Anderson *et al.* the first researchers that supply evidence of the stochastic as well as CSC model. They proved the existence of genetic diversity of cancer propagating cells and the variation of the genetic diversity with the developing state of disease.[26, 27] Notta *et al.* had similar results.[26, 28]

Due to the small number of cancer stem cells in total cell bulk, these cells need to be separated for further investigations. So far CSC isolation is carried out through their specific markers with different approaches. Four common methodologies will be described below: fluorescence-activated cell sorting (FACS) for CSC specific surface markers, Hoechst 33342 staining of distinct cells, sphere formation assay and measuring aldehyde dehydrogenase (ALDH) activity.

CSC isolation by expression of surface markers (membrane proteins):

The most often used and investigated surface markers are CD 133, first discovered in glioblastomas, and CD44 together with CD24 originally described in breast cancer CSC populations. Al-Hajj *et al* was the first, who discovered a $CD44^+/CD24$ CSC population in solid tumours.[15] Examples for other CSC surface markers are shown in table 1. Because of the fact that surface markers are also expressed in some other non-cancer cells or they are not present in every CSC cell, a combined use of more than one surface marker is recommended. Finally, surface markers can be used to enrich CSC positive cells, but a correlation of them with functional aspects of CSCs has to be improved.

Table 2 CSC surface markers found in different human solid tumours

Marker	Tumour	References
$CD44^+/CD24^-$	Breast cancer	28
$CD133^+$	Glioblastoma	15
$CD20^+$, SP	Melanoma	29
$CD44^+/\alpha_2\beta_1^{hi}/CD133^+$	Prostate cancer	30, 31
Side population	Ovarian cancer	32
$CD44^+$, Side population	Gastric cancer	33
$CD133^+$, Side population	Lung cancer	22
Side population, $CD44^+$	HNSCC	34

Side population assay:

One of many options to support the isolation of distinct CSC populations with surface markers is the so called “side population (SP) assay”.

Thereby, Hoechst 33342 dye is used to stain cells and isolate SP, which is poorly stained. The reason for low Hoechst staining is a dye efflux mediated by ATP-binding cassette (ABC) transporters. These transporters work inter alia as pumps to detoxify cells by disrupting cytotoxic agents from cells. In SP the ABC transporter is up-regulated leading to the poor staining with Hochst 33342. This population has been shown to bear stem cell characteristics.[35]

ALDH assay:

The ALDH super family encoding enzymes are responsible for detoxification mechanisms in the body and are liable for resistance to chemotherapeutic agents. Elevated ALDH activity has been shown in CSCs of breast, colon, and lung cancers.[36] After isolation of $ALDH^+$ population an enhanced spheroid formation has been observed. Therefore, in cancer stem cell research ALDH is widely used as a marker to isolate subpopulations. ALDH1 is the most investigated enzyme because of its prevailed appearance in various solid tumours.[36] $ALDH^+$ populations were plated into ultra-low attachment plates and showed an increased multicellular spheroid formation.[37]

Clonogenic and sphere-formation assays

The nature of CSCs is the ability to develop a tumour starting with one cell. Thus, cultured CSCs should be capable to form colonies from a single cell and to grow as spheres more efficient than other cells of the tumour bulk. Generally, the assay is based on evaluation of self-renewal capacity of tumour cells and the capability of growing in a non-adherent environment.[38]

In conclusion, to isolate a distinct CSC population, it is necessary to perform more than one methodology.

1.3. Cancer stem cells SCs in NETs

There is limited knowledge about the presence of CSCs in NETs. Gaur *et al.* found CSCs in gastrointestinal neuroendocrine surgical specimens and in the CNDT2.5 NET cell line (human midgut carcinoid) and demonstrated CSC properties by *in vitro* sphere-formation and *in vivo* tumourigenicity assays.[39] A number of potential CSC markers have been identified in NETs by many research groups, like Oct-4 in NETs of the ileum[40] and Nestin in small-cell lung cancer. Hence, it is necessary to invest more resources to study CSCs in NETs.

1.4. GI-NET cell lines as useful tools

Cell lines originating from neuroendocrine NETs represent useful experimental models for cancer research; above all proper cell lines are indispensable for establishing new therapeutic strategies. To date, different NET-derived cell lines have been developed and characterised, a remarkable number at the Institute in Graz by Roswitha Pfragner and colleagues. The SI-NET cell line P-STS was established from the primary tumour of a small intestine metastatic human carcinoid of a 42-year-old male. The existence of CSCs was not observed yet.[6]

1.5. Hypothesis & Aim

The hypothesis of my work is that NETs contain a subpopulation of cells termed neuroendocrine cancer stem cells that are responsible for malignant properties of NET tumours, in particular for cell invasion and the induction of angiogenesis.

The specific aims of this study are:

1) To find a feasible way to detect, characterize and isolate the CSCs in P-STS cell line derived from a small intestinal NET

2) To further analyse the malignant properties of these NET CSCs in chick chorioallantoic membrane assay

2. MATERIALS & METHODS

2.1. P-STS cell line

The SI-NET cell line P-STS was established from the primary tumour of a small intestine metastatic human carcinoid of a 42-year-old male. The primary tumour was localized in the terminal ileum. P-STS cells formed loosely attached monolayers in conjunction with numerous floating cells as well as adherently growing cells and cell clusters anchored to the adherent monolayer. The population doubling time was 4 days with formation of dense aggregates. Previous morphological and immunocytochemical investigations of the cell line showed characteristic markers of small intestinal carcinoids (pancytokeratin, cytokeratins 7, 8, 18 and19, serotonin (5-HT), NSE, CD56, protein gene product 9.5 (PGP9.5), calcitonin, synaptophysin, and gastrin-releasing factor). The ultrastructure exhibited the typical neuroendocrine granules together with hyperplastic Golgi areas indicating secretory activity on the part of these cells. A significant level of 5-HT (serotonin) secretion was detected *via* immuncytochemical and immunogold electron microscopy. Furthermore, the most frequent *menin*-gene mutations were not observed, but chromosomal aberrations were indicated at 18q and clonal tetraploidy was found. Most likely, the tumour occurred sporadically and not due to a mutation in the men1-gene.[6]

2.2. Cell culture conditions

P-STS cells grow semi-adherently. They were maintained in Ham's F12:M199 (1:2) medium with 10% fetal bovine serum (FBS) (Biochrom superior), 100 IU penicillin/ ml and 100 µg streptomycin/ml (P/S)(Sigma Aldrich) at 37°C and 5% CO_2. The cells were seeded with a starting concentration of $2x10^5$ cells/ml in cell culture flasks (Sarstedt, Austria), fed with additional 10 ml on day 4 and passaged on day 7: Cells were mechanically dissociated with a scraper from the surface and centrifuged at 180 *g* for 5 minutes. The cell pellet was then resuspended in 3 ml fresh medium and cell number was counted by Casy cell counter. Cells were then seeded with a concentration of $2x10^5$ cells/ml in new cell culture flasks.

2.3. Cell counting with CASY-system

To assess the exact cell number required for experimental setup, an electronic CASY-1® Cell Counter & Analyzer TTC (Schärfe Systems, Reutlingen, Germany) was used. The working principle is based on resistance measurement between an intact cellular membrane (viable cells) and a disrupted one. The cells were suspended in an electrolyte buffer (CASYton®) and were aspirated through a precision measuring capillary of a defined size. The measuring capillary featured two platinum electrodes to which a low voltage field was applied. Cells passing through the capillary result in a pulse signal which can be measured and further analyzed. A clear-cut differentiation between cell debris, dead cells, viable cells and volume differences can be made.

2.4. Spheroid formation - Ultra low adhesion plates

To confirm the ability of self-renewal, a defined characteristic of CSC, tumour spheres were generated. Single cell suspensions were seeded in ultra-low-adhesion round bottom 96-well plates (Costar® cell culture plates) containing 7500 cells/well cultured in Ham's F12/M199 (1:2) medium supplemented with 10% FBS. Observation duration lasted 10 days; pictures were taken on days 1, 4, 6, 8 and 10. The efficiency of spheroid formation was 100 %, each well contained one sphere (see Figure 11).[41]

2.5. RNA expression analysis

2.5.1. RNA isolation

Total RNA was isolated with the QIAGEN RNeasy Mini kit (QIAGEN, Netherland) according to the manufacturer's instructions.

The method combines the selective binding properties of a silica-based membrane with the speed of microspin technology. At first cell pellets were lysed and homogenized in the presence of a highly denaturing guanidine-thiocyanate–containing buffer (Buffer RLT), which immediately inactivates RNases to prevent the degradation of intact RNA. Ethanol is added to provide appropriate binding

conditions and the sample is then applied to an RNeasy Mini spin column where the total RNA binds to the membrane and contaminants are efficiently washed away. RNA is then eluted with 30–100 µl water.

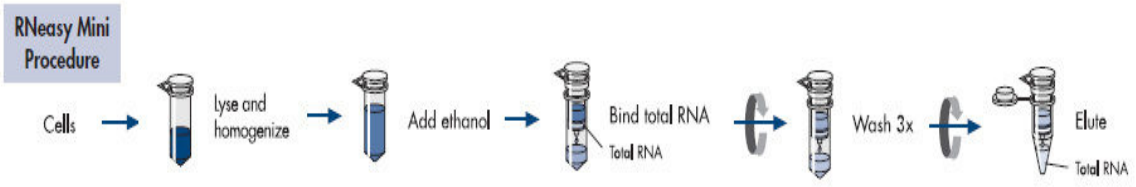

Figure 4 Single steps of the procession of QIAGEN RNeasy Mini Kit (Handbook QIAGEN RNeasy Mini Kit, Netherland, June 2013, fourth edition)

2.5.2. RNA quantification

To evaluate the quality and concentration of the total isolated RNA, a NanoDrop© ND-1000 Spectrophotometer (Thermo scientific, USA) was used. The quality was investigated by optical density measurements (A260/280 ratio of > 1.9). The NanoDrop© is a full-spectrum spectrometer that measures samples with high accuracy and reproducibility.

The OneStep RT-PCR Kit of QIAGEN I used offers the advantage that reverse transcription, conversion of RNA into cDNA, and PCR are carried out in the same tube.

2.5.3. Semiquantitative RT-PCR

The QIAGEN OneStep RT-PCR Kit was used to screen the CSC gene expression of the P-STS cell line.

This kit combines the reverse transcriptase and the PCR reaction in one tube. The specifically designed enzyme conducts both steps. A HotStart Taq polymerase conducts both steps. One of the benefits of a Hot Start Polymerase is the elimination of non-specific priming, avoidance of primer pairing and an increased product yield.

To perform a polymerase chain reaction with the OneStep RT-PCR Kit, a master mix, the components of which are listed in Table 3, was prepared in an autoclaved 1.5 ml tube. Two µL RNA or water were transferred into PCR tubes, aliquots of the master mix were added and the reaction vessels were centrifuged. The PCR cyles were performed using an iCycler (Bio-Rad, Hercules, CA, USA).

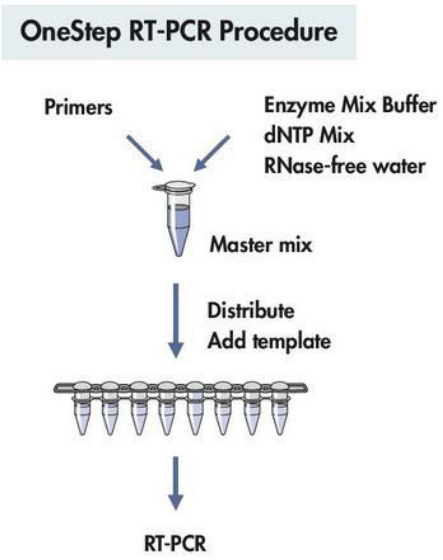

Figure 5 Schematic diagram representing relevant steps of the OneStep RT-PCR Kit

The PCR products were diluted with 6 µl Loading dye and 5 µl d_2H_2O. Components of the 2% agarose gel are shown in Table 6. 10 µl of each product were analysed via gel electrophoresis 60 mA, 100 V for 30 minutes (used 1x TAE buffer (Table 7)). A picture was taken, shown in Figure 8.

Table 3 Reaction components for OneStep RT-PCR

Components of Master mix	Volume/reaction [µl]
RNAase-free water	11.6
5x QUIAGEN OneStep RT-PCR Buffer	4
dNTP Mix	0.6
Primer A [30µM]	0.4
Primer B [30µM]	0.4
QUIAGEN OneStep RT-PCR Enzyme Mix	0.8
RNA or Water (negative control)	2
Total Volume	20

Table 4 Cycling conditions for OneStep RT-PCR

	Temperatur	Time [min]
Reverse transcription	50°C	30 min
Initial PCR activation step	95°C	15 min
27x following 3-step cycling		
Denaturation	94°C	1 min
Annealing	60 / 63 °C	1 min
Elongation	72°C	1 min
Final elongation	72°C	10 min

Table 5 Ingredients of 1kb DNA Ladder form Invitrogen

Substrate	Amount
Tris-EDTA (TE) 1x pH8,0	750 µl
Loading Dye Promega	200 µl
100 bp Ladder Invitrogen	50 µl

Table 6 Gel pipetting scheme for a 2% Agarose Gel

Substrate	Volume/Gel
Agarose	3 g
TAE Buffer (1x)	150 ml
GelRed™	6 µl

Table 7 Ingredients of the 50 %TAE buffer

Substrate
2 M Tris 0.05 M EDTA 57.1 ml glacial acid
Set pH to 8.5 and fill it up to 1 liter bidestilled water. Has to be diluted before using.

2.5.4. Quantitative PCR

The quantitative PCR (qPCR) allows the detection and measurement of PCR products without the need for gel electrophoresis. The whole procedure consists of

two-steps: The reverse transcription and the real time PCR (monitoring during the PCR). The isolated RNA was reverse transcribed into cDNA, which was then used as a template source for multiple real time PCR reactions. By the usage of SYBR Green (Biorad), an intercalating dye for double-stranded DNA, the amount of amplification product could be measured.

2.5.4.1. cDNA synthesis

The isolated RNA samples of the single cells and the long-term cultivation (three weeks) were reverse transcribed into cDNA. A High Capacity cDNA Reverse Transcription Kit (AB Life Tech Austria, Vienna) in combination with random hexamer primers was used for the reverse transcription step. The protocol starts with 10 minutes at 25°C followed by the reverse transcription step for 120 minutes at 37°C and the enzyme inactivation for 5 sec at 85°C. The cDNA was diluted 1:20 with nuclease free water before performing qPCR.

2.5.4.2. qPCR

For the qPCR step a master mix was prepared containing 4 µl of diluted cDNA (5 ng/µl), 7.5 µl iQ SybrGreen Supermix (Bio-Rad Laboratories, Vienna), 0.2 µM forward and reverse primer (see Table 8 for further information). Nuclease free water was used to fill the master mix up to a total volume of 15 µl. All samples were run in triplicates. MMP12 expression was measured with CFX96 from BioRad under the following conditions: step 1: 95°C for 3 min (enzyme activation), step 2: 95°C 10 sec, 60°C 30 sec, 72°C 10 sec; 40 repetitions; step 3: 95°C 30 sec; 55°C 30 sec followed by a melt curve analysis from 55°C to 95°C in 0,5°C steps every 5 sec. Triplicates with a standard deviation <0,31 were used for data analysis. Reverse transcription (RT) negative control (NTC) and no template control were included at each plate. For data analysis ΔΔCq-method was used.[42] Therefore the mean C_T values were normalized to the tested reference gene Hprt1 (forw: GACCAGTCAACAGGGGACAT, rev: CTGCATTGTTTTGCCAGTGT, 111bp) Following the normalization of the test sample (spheroid) to the calibration sample (single cells), the expression ratio was calculated to get the relative gene. (Real time applications guide Biorad)

Table 8 Primer Sequences used for OneStep RT-PCR and Real time PCR

Gene Bank	GeneID	Gen name	Pimer (5' – 3')	Anneal. Temp. (°C)	Cycles	Product Size (bp)
NM_006474	PDPN	Podoplanin	TGACTCCAGGAACCAGCGAAG GCGAATGCCTGTTACACTGTTGA	63	30	86
NM_002033	CD 15	3-fucosyl-N-acetyl-lactosamine	GCAGGTGGGACTTTGTTGTT CCAAGGACAATCCAGCACTT	60	30	150
NM_006617	Nestin	Nestin	AGCGTTGGAACAGAGGTTGGA TGTTTCCTCCCACCCTGTGTCT	63	30	549
NM_002442	MSI-1	Musashi-1	GGTTTCCAAGCCACAACCTA TCGGGGAACTGGTAGGTGTA	60	30	74
NM_005180	BMI-1	Polycomb complex protein	AACAATGGAATATGCCTTCTCTGC ACTGGGGACAATGAAATGTTTAGC	60	30	263
NM_003106	Sox-2	Sex-determining region Y-box2	CAAAGAAAAACGAGGGAAAT ATGGGATTGGTGTTCTCTTT	60	30	166
NM_002165	ID-1	inhibitor of DNA binding 1	GTAAACGTGCTGCTCTACGACATGA AGCTCCAACTGAAGGTCCCTGA	63	30	143
NM_001173531	Oct-4	octamer-binding transcription factor 4	AGCGATCAAGCAGCGACTATG CAGAGTGGTGACGGAGACAG	60	30	203
NM_001297698	Nanog	Homeobox protein NANOG	TTTGTGGGCCTGAAGAAAACT AGGGCTGTCCTGAATAAGCAG	60	30	116
NM_001145847	CD 133	prominin 1 (PROM1)	AGTCGGAAACTGGCAGATAGC GGTAGTGTTGTACTGGGCCAAT	60	30	99
NM_001257386	ABCG 2	ATP-binding cassette	CAGGTGGAGGCAAATCTTCGT ACCCTGTTAATCCGTTCGTTTT	60	30	247
NM_013230	CD 24	CD24 molecule	CTCCTACCCACGCAGATTTATTC AGAGTGAGACCACGAAGAGAC	60	30	166
NM_000222	CD 117	Mast/stem cell growth factor receptor	CGTTCTGCTCCTACTGCTTCG CCCACGCGGACTATTAAGTCT	60	30	117
NM_000692	ALHD	aldehyde dehydro-genase	GCACGCCAGACTTACCTGTC CCTCCTCAGTTGCAGGATTAAAG	60	30	129

2.6. Flow cytometry

Flow cytometry is an analytical technique for the determination of optical and fluorescence characteristics of single cells or particles. A laser beam is passed through a flowing suspension of the cells. If a labelled cell passes the laser beam, the fluorescent dye absorbs the energy and emits light at a higher wavelength. These light signals are detected by a photomultiplier and digitalized for computational analysis. The resulting information is usually delineated in a histogram or two dimensional dot-plot formats.[43]

The following properties can be measured with flow cytometry: cell size, granularity or internal complexity, fluorescent dyes bound on DNA, RNA, or a wide range of membrane-bound and intracellular proteins.

In this work cells were harvested and diluted in Phosphate buffered saline **(**PBS). Antibodies with a fluorescent dye were used for labelling (see Table 9).
Flow cytometer: BD LSR Fortessa™ (BD Biosciences, USA)

Table 9 Antibodies used for FACS analysis of CSC

Antibody target	Isotype	Label	Company	Catalog number
Human CD117	Mouse IgG1, κ	BV 421	BD Biosciences	562435
Human CD24	Mouse IgG2a, κ	PE	BD Biosciences	560991
Human CD133	Mouse IgG1	PE	MACS Miltenyi Biotec	130-098-826
Human CD44	Mouse IgG1, κ	PE	Biolegend	338807

2.7. Aldefluor assay

The Aldefluor assay is a method to identify aldehyde dehydrogenase (ALDH) activity in normal and cancer stem cells.
To stain the ALDH positive cell population, the Aldefluor kit (STEMCELL Technologies, Vancouver, CA) was used. Samples were subjected to the Aldefluor assay according to the manufacturer's protocol. The cell pellet was washed with PBS to remove the medium after mechanical dissociation. $1x10^6$ cells were re-suspended in Aldefluor assay buffer containing the ALDH substrate (BODIPY™-

aminoacetaldehyde (BAAA)). Half of the sample was treated with diethylaminobenzaldehyde (DEAB; an ALDH inhibitor) as a negative control. Both samples were incubated at 37°C for 30 minutes. Cells expressing high levels of ALDH become brightly fluorescent (ALDHbr) and can be identified using a flow cytometer.[39]

2.8. Chorioallantoic membrane assay

The chorioallantoic membrane (CAM) assay takes advantage of the highly vascularized extra-embryonic membrane of the avian embryo to analyse several aspects of tumour biology. This model system allows extensive analysis of tumour cell intravasation, tumour cell colonization or tumour-induced angiogenesis. Thus, the natural immunodeficiency and the blood vessel network provide best conditions for sustaining grafted tissues and cells without species-specific restrictions. The chorioallantois is resulting from the fusion of the allantois and the chorion which is occurring between days 4 and 5 of embryonic development. The main function of the CAM is the gas exchange between the embryo and the egg shell (Romanoff, 1960), moreover, it also plays a role in the storage of excretions, electrolyte transport and mobilization of calcium from the shell for mineralization. At day 10 of embryonic development the vascular CAM network is sufficiently established, thus allowing successful xenotransplantation of cells or tissue.[44-47]

For tumourigenesis studies with the CAM assay two slightly different procedures are possible: the *ex ovo* cultivation and the *in ovo* cultivation. Because of a better accessibility for manipulation and direct visualization of the developing xenografts on CAM, the *ex ovo* shell-less cultivation was selected.[48]

The procedure consists of four main steps as shown in Figure 6.
In short, the delivered fertilized White Leghorn chicken eggs (local chicken farm Schropper, Gloggniz) were cleansed with warm water and wiped with a tissue soaked in 5% H_2O_2 before incubation in a rotary thermostat at 37.6°C and 40-60% humidity. On day 3 the eggs were cracked with a wide wheel of a drill, which gently notched three quarters of the egg shell in equatorial direction. The content was transferred into a sterile weighing boat and covered with a plastic petri dish. Eggs were incubated for another 7 days.[48]

On day 10 3 - 4 silicon rings of 0.5 mm diameter/egg were placed on the CAM. These rings act as a border for the xenografts. Per egg, 2-4 onplants with cells or spheroids suspended in 10 µl medium (with or without Matrigel™ at a 1:2 ratio) were pipetted in the centre of the ring. After another 3 days of incubation, the first transplants were photographed (Fluorescence Stereomicroscope SZX16 with transmitted light unit, Olympus) and harvested. Thereafter every day several eggs of one condition were harvested.[48]

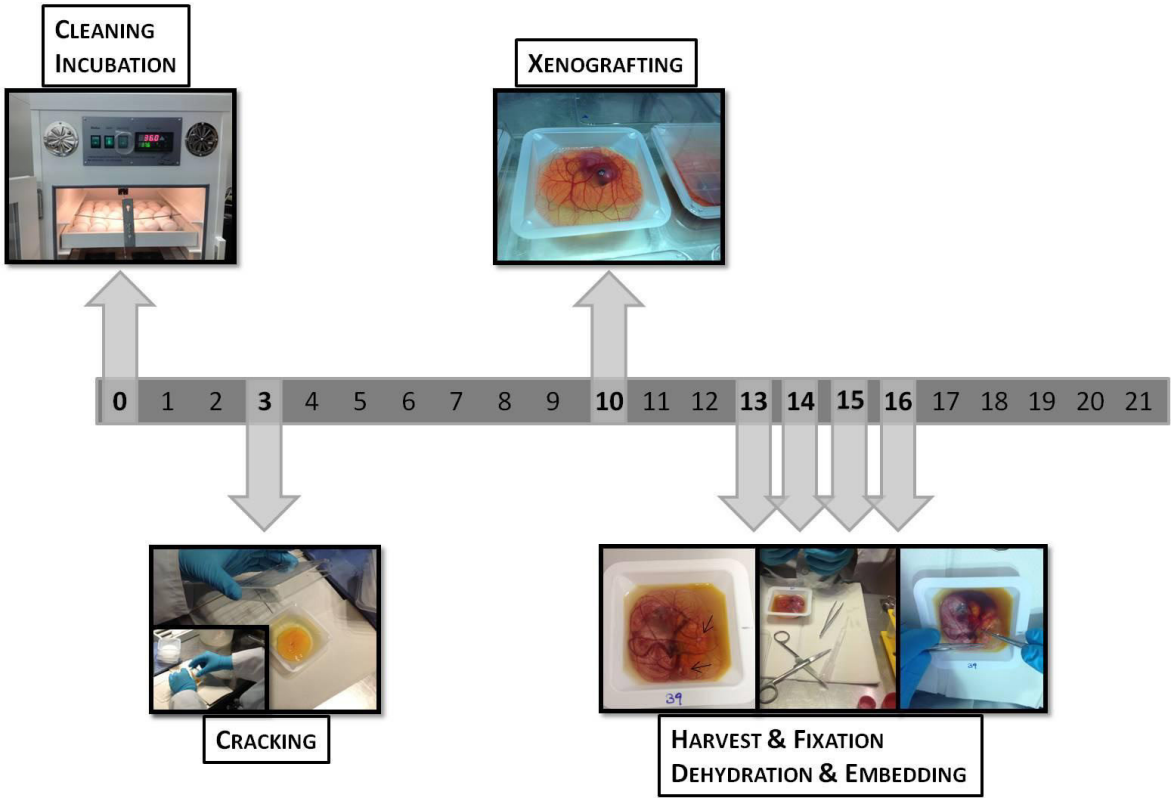

Figure 6 Timetable and experimental setup of the shell-less CAM assay.

2.9. Histological analysis of spheroids & CAM

To investigate the spheroid formation and the xenograft invasion histological analyses were performed.

Spheroid:

Six day old spheroids were harvested using a 1000µl pipette and transferred to a 1.5 ml tube. After letting them sink to the bottom of the tube, the medium was removed. Fixation in Paraformaldehyde (PFA) required 1-2 hours. Thereafter, dehydration was performed by incubation in alcohol solutions with increasing concentrations followed by incubation in a toluene solution (Table 10). Then the spheres were put into paraffin no. 6 and 9 for 15 min each. Finally, tissue molds were used to embed the spheres into paraffin.

Histological sections were made with microtome (Leica Biosystems, Austria) and stained with haematoxylin (RAL Diagnostics, France) and eosin (Merck Millipore, Germany) (H&E) staining.

Tissue:

At different time points after grafting, onplants with the underlying tissue were cut out with fine scissors and washed in PBS. Then, onplants were transferred into small petri dishes filled with 3 ml PFA (fixation time: 16 hours). The duration of the following alcohol and toluene steps as well as the paraffin steps are shown in Table 10.

Table 10 Duration of dehyration steps for spheroids and onplant embedding

Reagents	Duration spheroid (min)	Duration onplant (min)
70% Ethanol	15	30
95% Ethanol	15	30
95% Ethanol	10	15
100% Ethanol	15	30
100% Ethanol	10	15
Toluene	15	30
Toluene	10	15
Paraffin #6	15	30
Paraffin #9	15	30

Tissue molds were used to embed the onplants vertically. Tissue orientation: tumour left handed.

2.10. Immunohistochemistry

Immunohistochemistry (IHC) is a method to detect specific molecules fixed on tissue slides by exploiting the principle of Antigen-Antibody interaction. The indirect IHC, used in the experiments, utilizes one antibody against the antigen being investigated and a second, labelled antibody to bind the first antibody. The indirect method involves an unlabelled primary antibody (first layer) which reacts with tissue biomarker, and a labelled secondary antibody (second layer) which reacts with the primary antibody. Cells or tissue were fixed with paraformaldehyde (PFA) and embedded in paraffin, which has to be removed *via* treatment with xylene followed by alcohol solutions of different concentrations. Proteins of tissue or cells were now accessible for antibody staining. (see Table 11 for the list of antibodies) For the Immunohistochemical staining the ab64264-Mouse and Rabbit Specific HRP/DAB (ABC) Detection IHC kit from abcam® (England) was used. Steps were performed

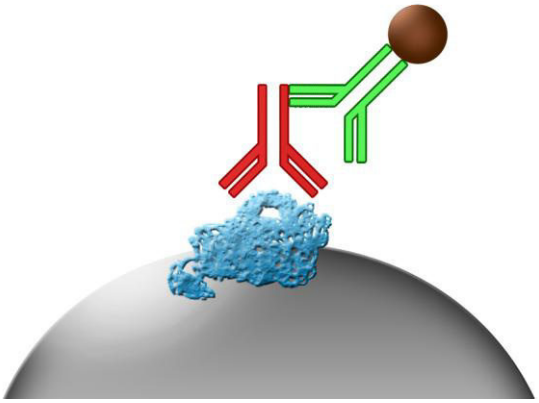

Figure 7 Illustration of indirect IHC method

as described in the manual. See supplement /supporting information for further details.

Table 11 List of used antibodies and dilution for the CAM section staining

Antibody target	Isotype	Company	Catalog No	Dilution
Chromogranin A	Polyclonal Rabbit IgG	ThermoFisher Scientific	RB-9003-P	1:500
Synaptophysin	Mouse IgG1	ThermoFisher Scientific	MA5-11575	1:120
Cytokeratin	Mouse IgG1, kappa	Dako	M351529	1:200
Desmin	Mouse IgG1,kappa	Dako	M076029	1:80
Ki 67	Mouse IgG1, kappa	Dako	M724029	1:80

3. RESULTS

3.1. Expression analysis of CSC makers in P-STS

3.1.1. P-STS cell line processes CSC sub-population

In order to determine the stem cell characteristic of P-STS cell line expression of CSC specific genes were observed by semi quantitative RT-PCR. The CSC specific genes belong to different main groups: regulatory core transcription factors (Nanog, Sox2, Oct4[49]), surface makers (CD133, CD24, CD117; CD15), ALHD and ABCG2 which represent hosts of detoxification processes, proteins correlated to cell growth and proliferation (MSI1, BMI1, ID-1), PDPN a transmembrane glycoprotein and Nestin a collagen VI intermediate filament expressed during invasion and metastatic processes.

The RT-PCR provides perfect conditions for screening the cell line through many different markers shown in Figure 8. BMI1 was found to be the most highly expressed protein. CD 24, CD117, ID-1, CD133, Nestin, MSI, OCT4 and Nanog showed lower expressions. Only three of the tested genes (PDPN, CD15, SOX2) exhibited no expression.

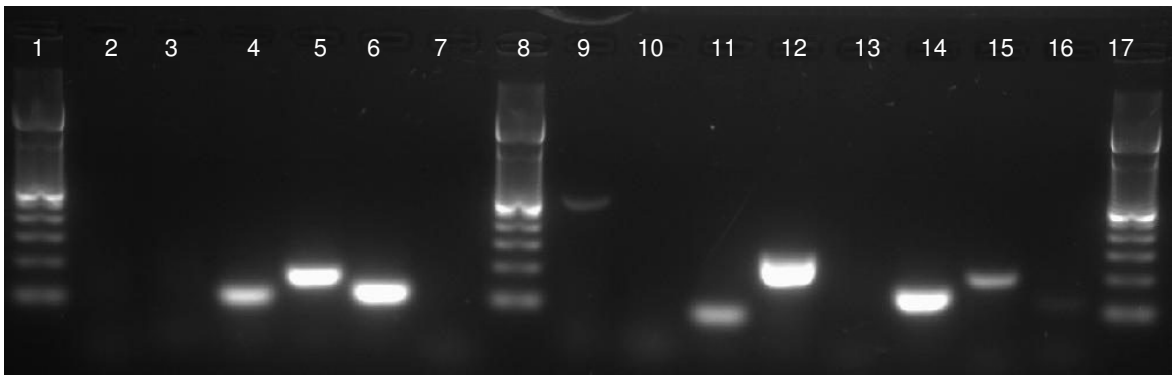

Figure 8 RT-PCR analysis of CSC marker expression at P-STS single cells: RNA of confluent P-STS cells were isolated. The QIAGEN RT-PCR kit was used to perform the PCR. The products were analysed via gel electrophoreses (2% agarose gel, 1%TAE buffer). 1 Ladder 100bp; 2 PDPN; 3 CD15 4 CD133; 5 CD24; 6 CD117; 7 ABCG2; 8 Ladder; 9 Nestin; 10 ALDH1; 11 MSI1; 12 BMI1; 13 SOX2; 14 ID-1; 15 OCT4; 16 Nanog; 17 100bp Ladder

3.1.2. Aldefluor Assay

Recent research has shown that ALDH is a promising indicator for the presence of CSC sub-population in many cancers.[39, 50-53] The P-STS cell line was analysed for the presence of ALDH activity using the Aldefluor assay kit (Stemcell technologies, Canada) via flow cytometry. Triplicates were performed. A population of 2.5% of the P-STS single suspension was found to express aldehyde dehydrogenase. This result supports the theory that only a small sub-population exhibits stem cell characteristics.

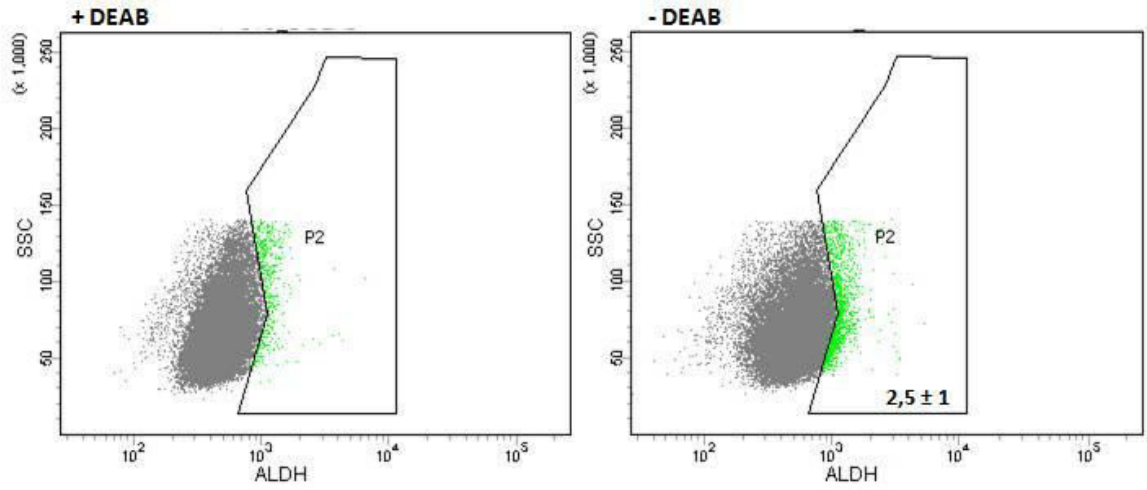

Figure 9 Identification of ALDH$^+$ cells in the P-STS cell line. Flow cytometric analysis of P-STS single cells suspension stained by ALDEFLUOR™ Kit from Stemcell technology. Dot-plots show ALDH$^+$ sub-populations in ‘‘-DEAB’’ (right panel) and the negative control, “+DEAB” (left panel). “+DEAB“ was used to set the gates defining the the ALDH expressing population (-DEAB). Data represents mean ± SEM from 3 independent experiences.

3.1.3. FACS – investigation of specific CSC surface markers

Currently, specific cell surface markers are used to isolate CSC sub-populations. However, none of these markers are exclusively expressed by CSCs. Therefore, a combination of two or more markers serves for a more precise identification of CSC population. The expression of four recurrent surface markers (Table 9) has been analysed by flow cytometry.

CD133, also known as Prominin-1, one of the most prominent objects of CSC research, has an expression level of almost 98% (see figure Figure 10).[29, 54]

Gastric cancer and breast cancer were found to have a sub-population expressing CD44 or a combination of $CD44^{+}/CD24^{-}$. The P-STS cell line does not express the CD 44 surface maker, but reveals 43,9 % of CD 24 expression.[33, 38]

CD 117 is a cytokine receptor on the surface of hematopoietic stem cells and identifies progenitor cells in the bone marrow. In addition, CD 117 were used to isolate CSC subpopulations in ovarian cancer. [55] 48% of the P-STS cell line showed the presence of the CD117 marker.

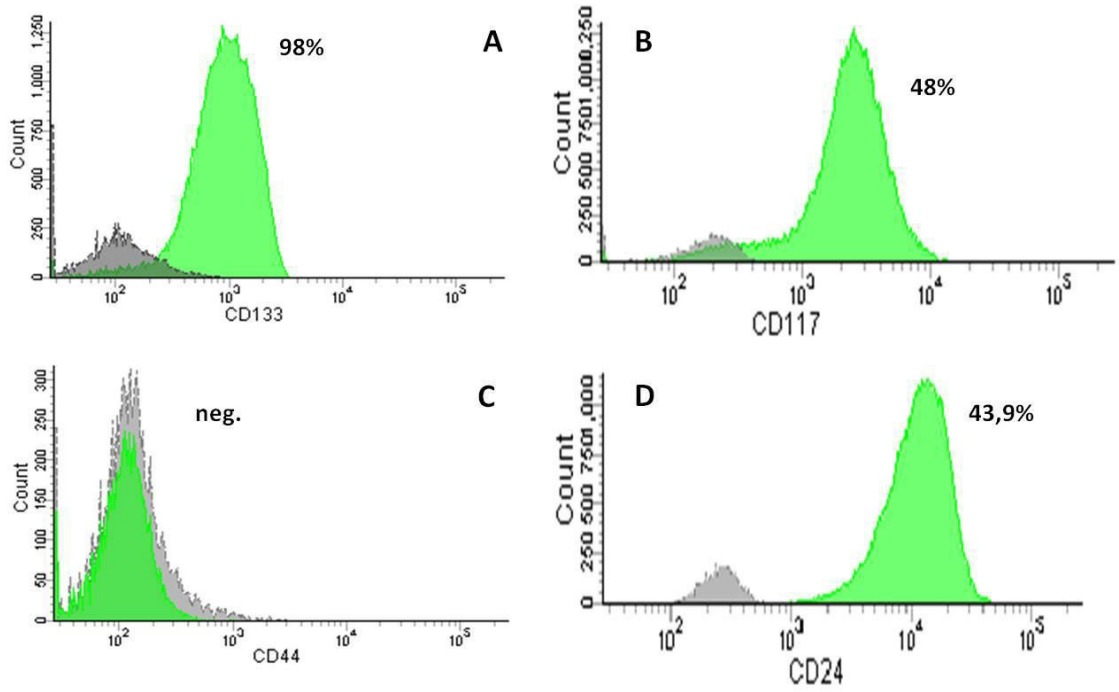

Figure 10 Expression of characteristic CSC markers in P-STS single cells assessed by flow cytometry. Cells were stained with BV- and PE-conjugated monoclonal antibodies against A: CD133, B: CD117, C: CD44 and D: CD24. The histograms from the flow cytomety analysis show the percentage of the positive cells (green) and the isotype control (grey).

3.2. Formation and cell growth in spheres

To confirm the ability of self-renewal, a defined property of CSC, tumour spheres were generated. Single cell suspensions were seeded in ultra-low-adhesion round bottom 96-well plates containing 7500 cells/well cultured in Ham's F12/M199 (1:2) medium supplemented with 10% FBS. Observation duration was over 10 days,

pictures were taken one day 1, 4, 6, 8 and 10. The efficiency of spheroid formation was 100%, each well contained one sphere. The cells start to form loose aggregates on day 1. Within 5 more days a round, compact and unbreakable sphere is formed. The cultivation up to day 10 leads to a decrease of the compact structure. (Figure 11) This makes it impossible to transfer the spheroid with a pipette tip without breaking it apart.

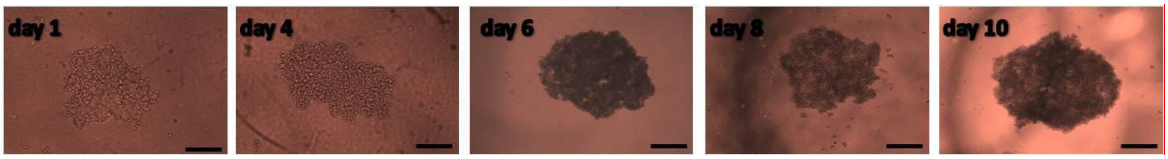

Figure 11 Spheroid formation of P-STS cell line: In a total volume of 200µl, 7500 cells were seeded into each well of the ultra-low-adhesion round bottom 96-well plates (Corning, Tewksbury, MA). Cultivation time lasted 10 days. On day 1, 4, 6, 8, 10 pictures were taken to investigate the growth and formation habit. Representative images of the spheroids by phase-contrast microscopy (×40). Bars = 500 µm.

3.3. Comparison of CSC markers in 2D vs 3D

Many publications are addressing the correlation between sphere formation ability, self-renewal potential and the existence of CSCs. Therefore, spheres, cultured for three weeks, were analysed on their relative gene expression refering to monolayer cultured cells by quantitative PCR.

Nanog, Sox2, and Oct4 are transcription factors (TF) regulating pluripotency and self-renewal in embryonic stem cells. The expression of Nanog, a downstream target of Oct4[56], and Sox2, Sry-containing protein[57], is 5.28 (Nanog) and 3.2 (Sox2) fold higher in spheres than in single cells. An overexpression of the aforementioned genes is associated with several carcinomas (e.g.pancreas, lung, esophagus and breast[56, 57]).

The gene expression of Oct 4, a member of the POU family[49], is decreased by a factor of 0.8 even though Nanog and Sox2 expression shows enhanced values.

ID-1, member of the inhibition of differentiation/DNA binding protein family, is another factor capable of self-renewal in embryonic stem cells.[58] The significantly higher expression of ID-1 is an additional indication of the acceleration of CSCs in spheres.

The overexpression of the transcription repressor BMI1, Musashi (MSI) a family member of neural RNA-binding proteins, and the IV IF protein nestin are commonly found in different tumour tissues. The elevated expression of these three factors (shown in Figure 12), which not only control cell signalling and proliferation, can also be found in other tumour cells (prostate tumour and glial tumours).[59, 60]

ABCG2, a member of the ATP-binding cassette (ABC) transporters superfamily, is a gene responsible for drug resistance when it is overexpressed. The three-week-old spheres have a lower ABCG2 expression, and therefore a lower drug efflux, than P-STS single cells.[61]

The surface markers of the spheres have an elevated expression compared to the single cell expression, except CD 133 and CD 15 which showed a decrease or same level of expression respectively. PDPN, a platelet aggregation-inducing mucin-like sialoglycoprotein[62] and ALDH showed the same expression level in sphere and single cells.

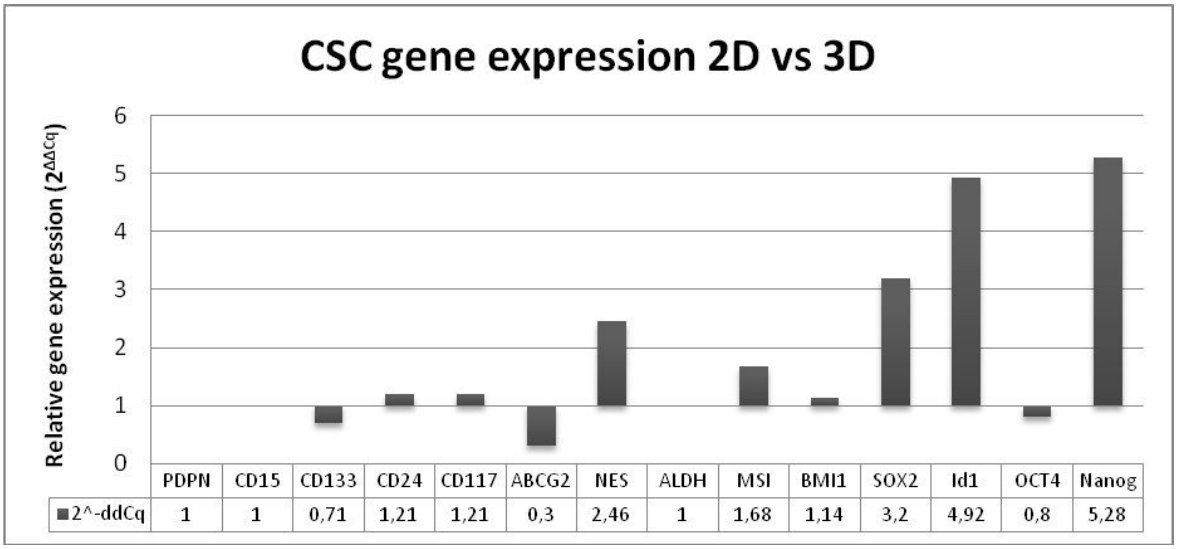

	PDPN	CD15	CD133	CD24	CD117	ABCG2	NES	ALDH	MSI	BMI1	SOX2	Id1	OCT4	Nanog
■2^-ddCq	1	1	0,71	1,21	1,21	0,3	2,46	1	1,68	1,14	3,2	4,92	0,8	5,28

Figure 12 Comparison of the cancer stem cell marker expression in P-STS single cells and spheres. Used genes listed in Table 8. The relative gene expression is the fold increase (decrease) of the target gene in the test sample relative to the calibrator sample and is normalized to the expression of the reference gene.[42] and relative gene expression was assessed using the ΔΔCq-method (n=3).[42]

3.4. CAM assay – xenografing of 2D vs 3D

To compare the different behaviour of P-STS cell line as single cells versus P-STS spheroids on tumour growth and invasiveness, the in vivo CAM assay was performed. For tumour xenografting 5 days old spheroids and single cells were grafted on the CAM of 10 day old chicks. Both experimental settings started with the same amount of cells, (2 spheroids comprising 7500 cells each and 15000 single cells) and were processed with and without Matrigel™. Figures 10-13 show the macroscopic tumour development of one setting of independent CAM assays in the course of 4 days. Interestingly, macroscopic comparison of spheroid and single cells with Matrigel™ showed no significant difference of the tumour size. The shape and density of the tumour seemed to differ from CAM experiment to CAM experiment, thus reflecting the individual tumour development. However, the trend of behaviour remains the same. The tumour growth of the experimental design without Matrigel™ confirms the assumption that spheroids are more invasive than single cells.

Only 3 xenografts created round-shaped tumour-like structures with the size of little pinheads or smaller. All the other onplanted cells built streaks around the inner corner of the silicon ring. Thus, single cells require Matrigel™ to have the ability to find together. On the contrary, spheroid onplants have the ability to form tumours roughly comparable in shape, density and size of single cell onplants with Matrigel™. The macroscopic comparison leads to the same result as the CAM experiment, namely the confirmation of the theory that spheroids are acting in a more invasive way. The increased aggressiveness is possibly the result of promoted tumourigenic factors which are unregulated in spheroids compared to single cells as shown above, Figure 12.

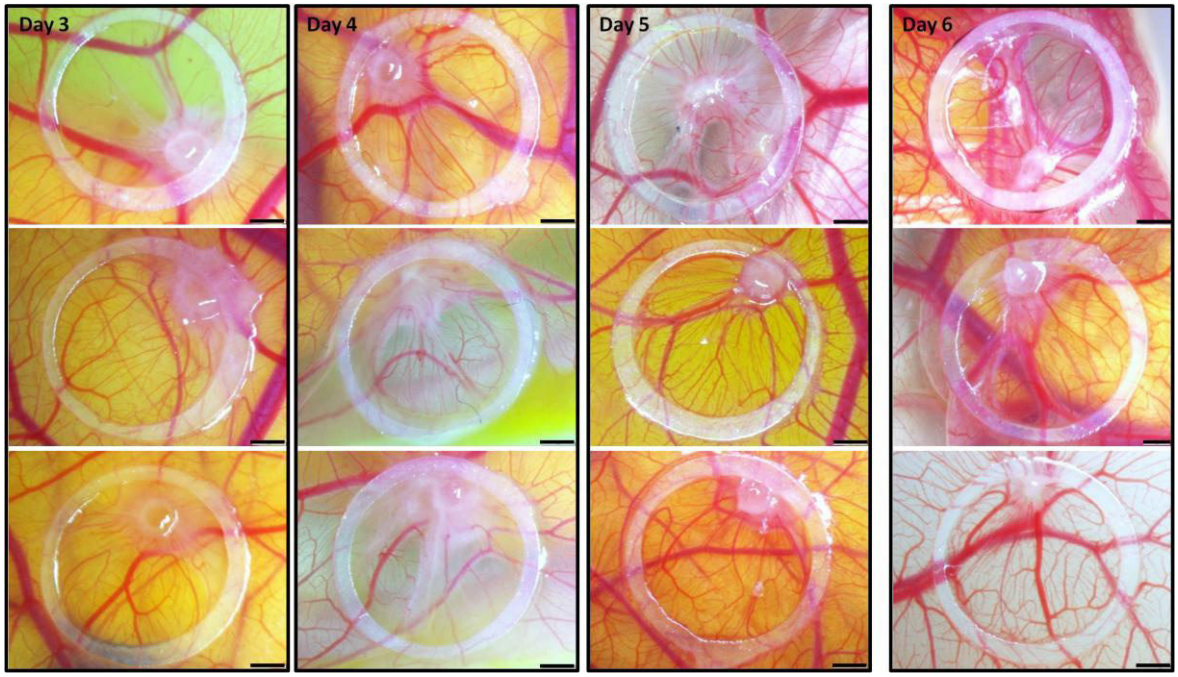

Figure 13 Macroscopic observation of xenografted P-STS spheroids on shell-less CAM assay. 5 days old spheroids (2x7500 cells) with Matrigel™ were implanted on CAM at embryonic day 10 and collected on day 3, 4, 5 and 6 after xenografting. n=3 Scale bar: 1mm

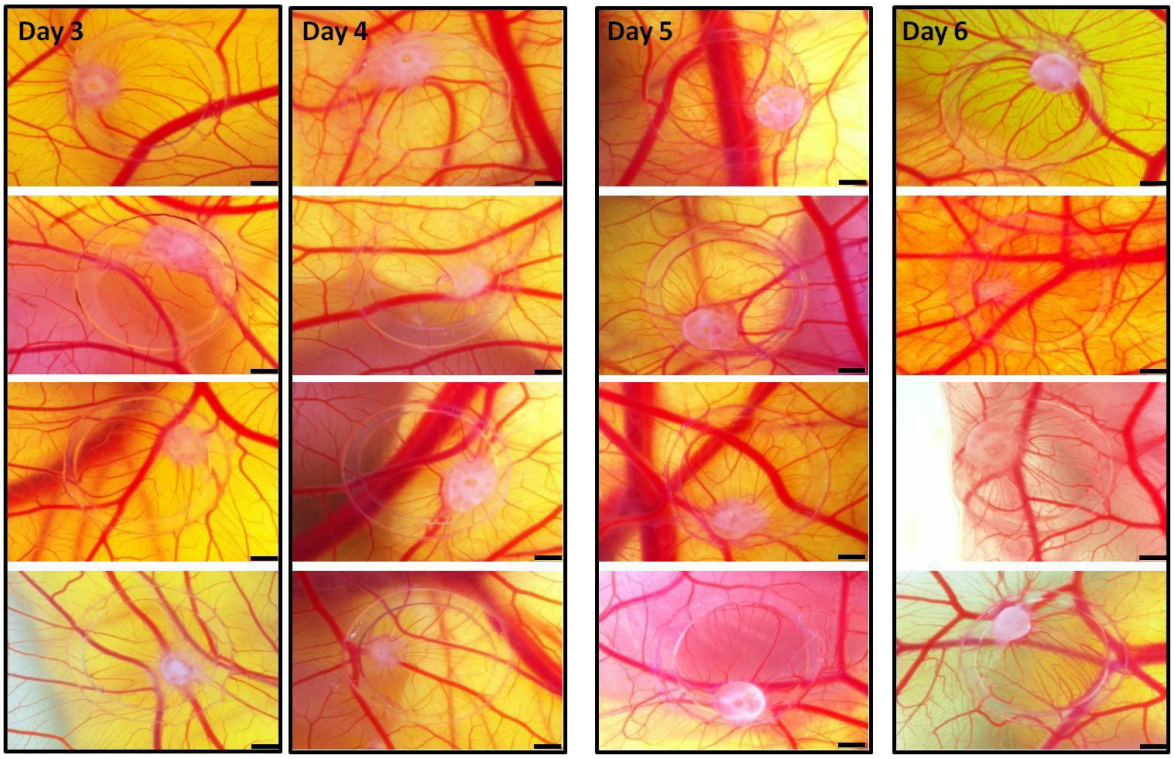

Figure 14 Macroscopic observation of xenografted P-STS single cells on shell-less CAM assay. Single cell suspension (15000 cells) was mixed with Matrigel™ ^{TM} and were implanted on CAM at embryonic day 10 and collected on day 3, 4, 5 and 6 after xenografting. n=4 Scale bar: 1mm

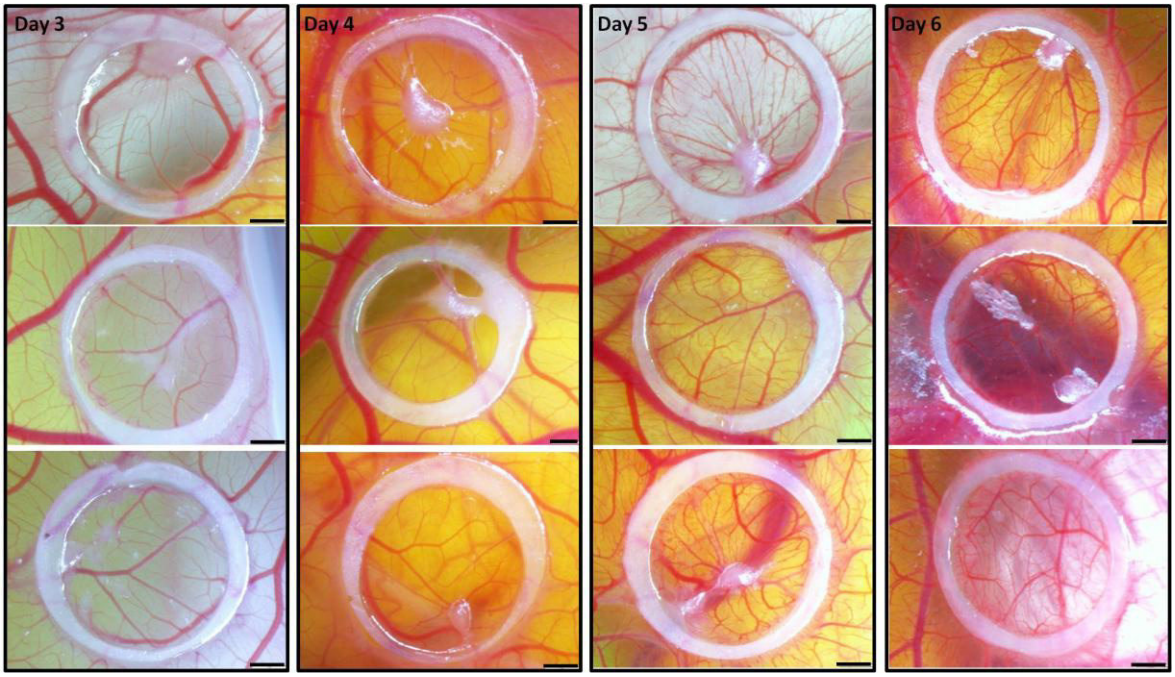

Figure 15 Macroscopic observation of xenografted P-STS spheroids on shell-less CAM assay. 5 days old spheroids (15000 cells) without Matrigel™ [TM] were implanted on CAM at embryonic day 10 and collected on day 3, 4, 5 and 6 after xenografting. n=3 Scale bar: 1mm

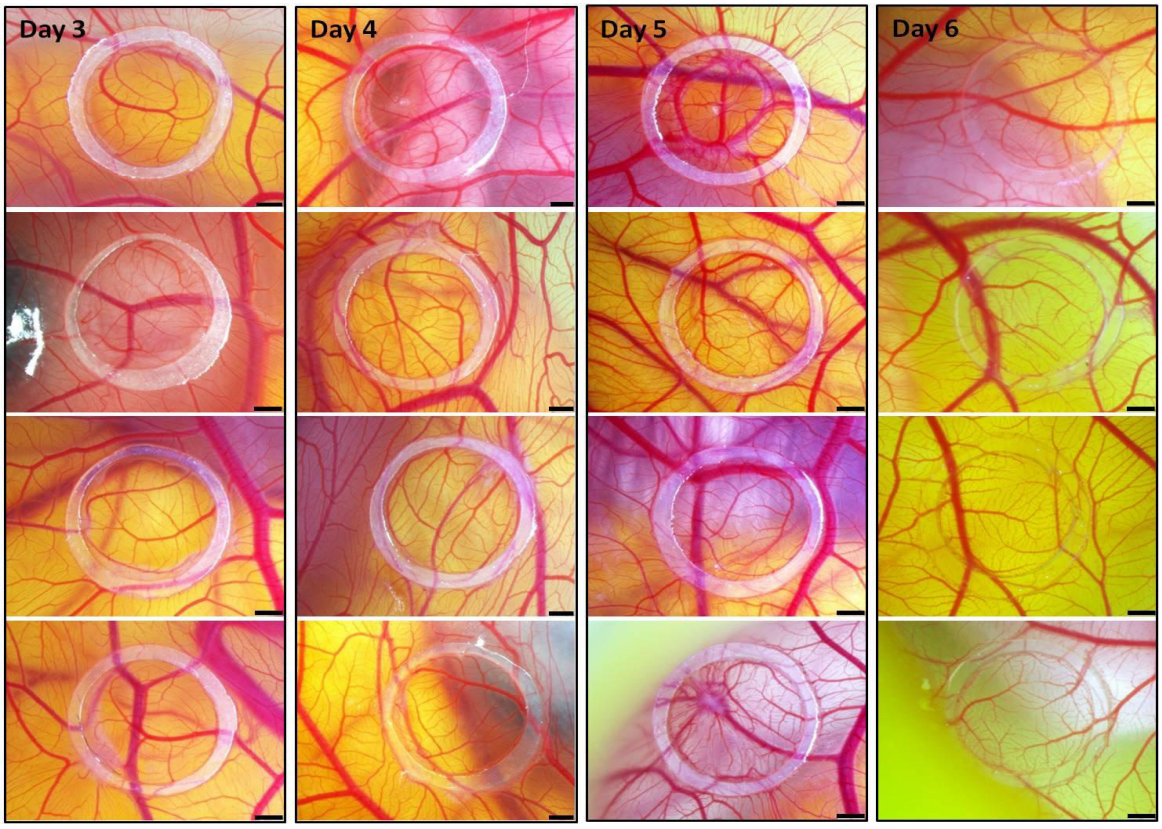

Figure 16 Macroscopic observation of xenografted P-STS single cells on shell-less CAM assay. Single cell suspension (15000 cells) was mixed without Matrigel™ [TM] and were implanted on CAM at embryonic day 10 and collected on day 3, 4, 5 and 6 after xenografting. n=4 Scale bar: 1mm

To determine the tumour growth and invasion capacity, histological sections and immunhistochemical staining of the processed CAM tissue were performed. Every 25th section was stained *via* H/E (shown in 17, 19, 21, 23, 26, 28, 29)

Immunhistochemical staining of 3 SI-NET markers, cytokeratin, synaptophysin and chromogranin as well as desmin (angiogenic activity) and Ki67 (mitotic marker) were used (shown in Figure 30).

Figure 17, 19, 21, 23, 26, 28, 29 show overviews through the whole embedded tumour tissue. Spheroids harvested on day 3 and day 6 without Matrigel^{TM} (Figure 28 & 30) showed a low invasion capacity of the tumour cells, but induced massive inflammatory reactions in the CAM (Figure arrows). The mentioned markers were expressed in both spheroids and single cells. Xenografted single cells without Matrigel^{TM} of the P-STS cell line, day 3, were able to invade in the CAM epithelium (shown Figure). Day 6 single cells without Matrigel^{TM} were not able to establish xenografts on CAM (Figure). Single cells and spheroids with Matrigel^{TM} showed an invasive tumour growth on day 3 as well as on day 6. (Figure 17, 19, 21, 23)

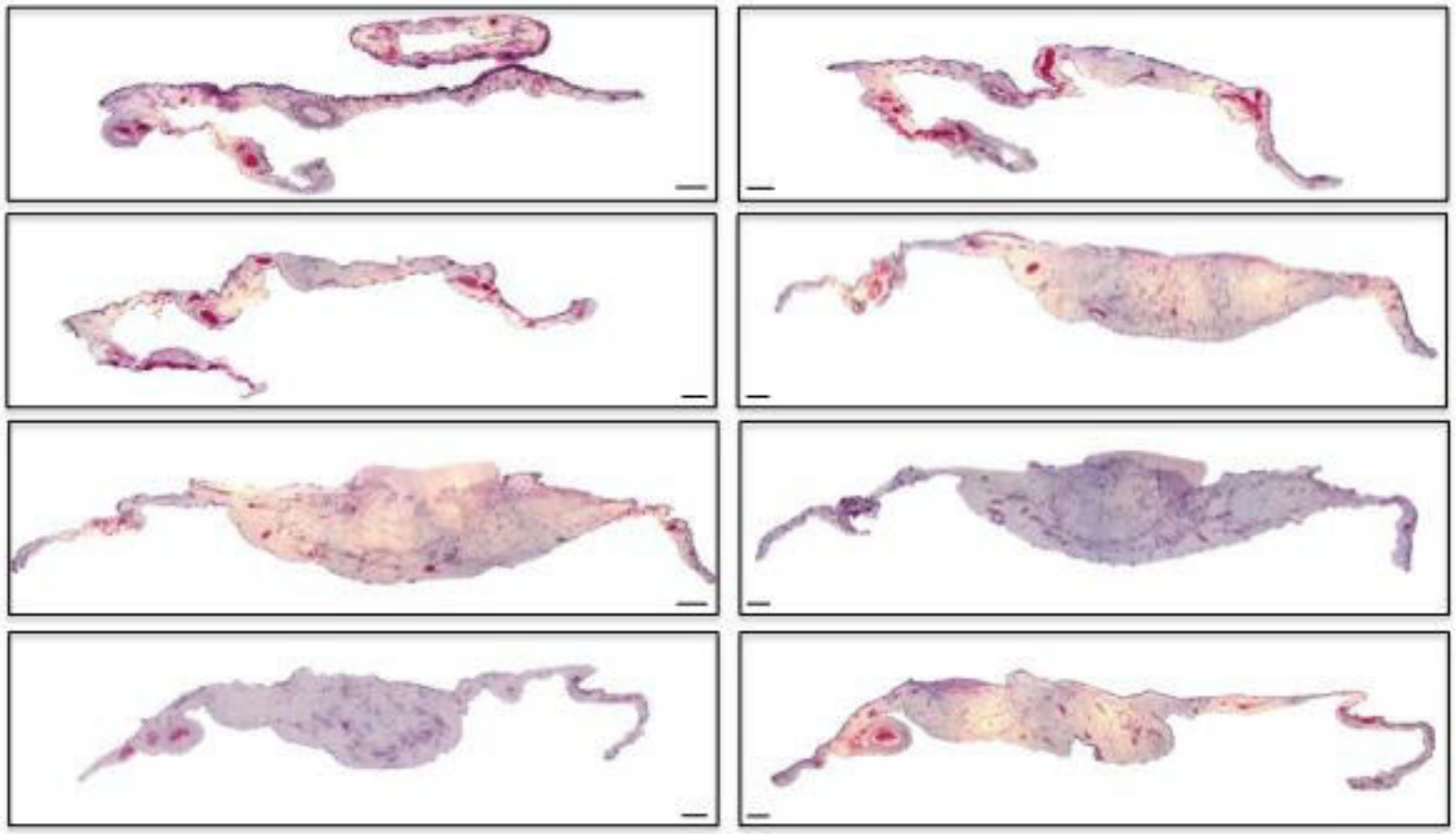

Figure17 Microscopic observation of histological sections through the developed tumour of single P-STS cells with Matrigel™. After 3 days of tumour development on CAM the accrued xenograft was processed through histological fixation and paraffin embedding. Each 25th 5µm thick section was stained with H/E. Overview through the whole tumour. Bar:200µm

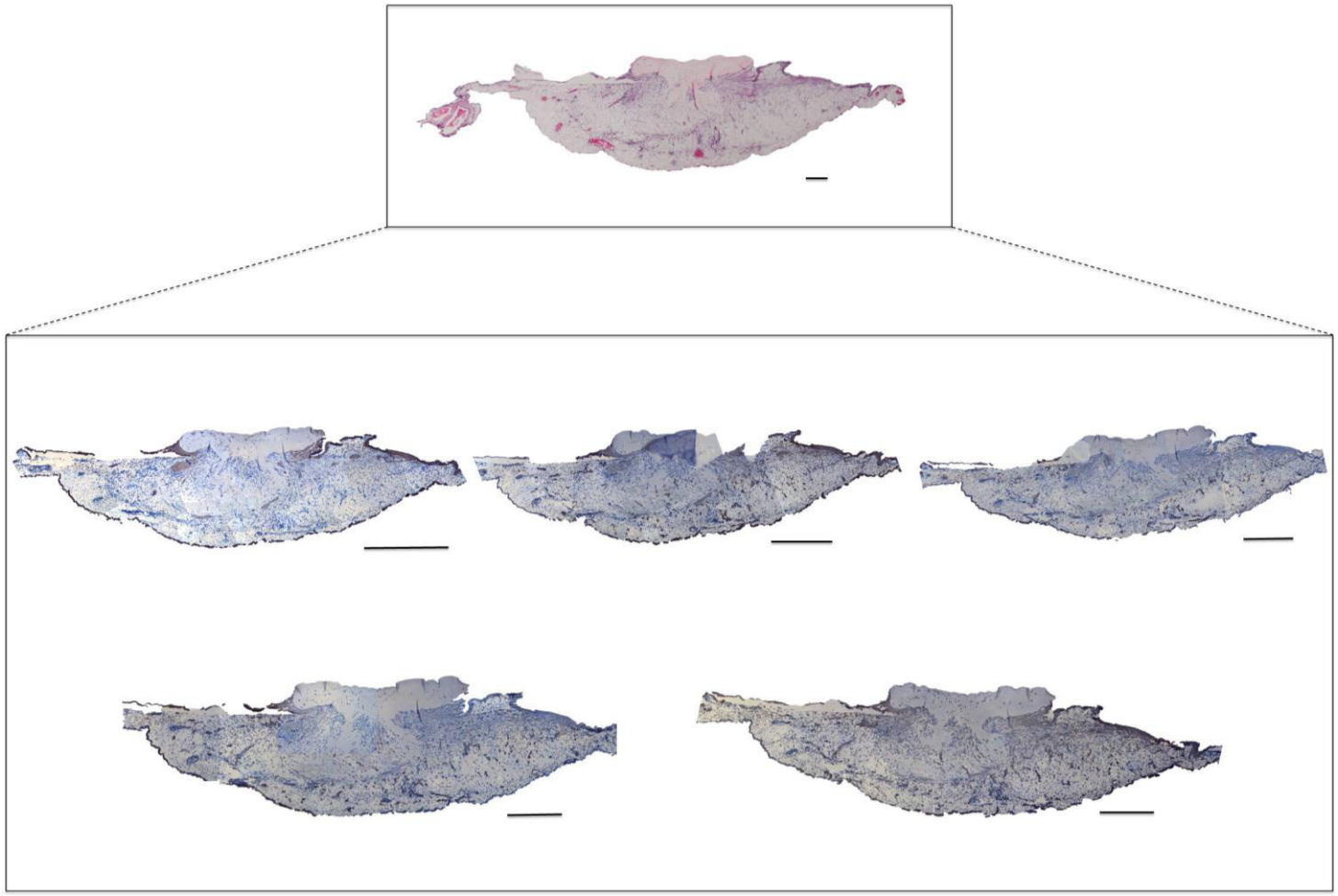

Figure18 Histological sections of 3 days old tumour xenograft of P-STS single cell with Matrigel™ stained with SI-NET markers (cytokeratin, synaptophysin, chromogranin), Ki-67 (mitosis marker) and desmin. 3 days after xenografting the developed tumour was processed through histological fixation and embedding procession steps. 5µm thick sections were cut and stained chronologically from top to down: H/E staining, cytokeratin, desmin, Ki-67, synaptophysin and chromogranin . Scale bar:200µm

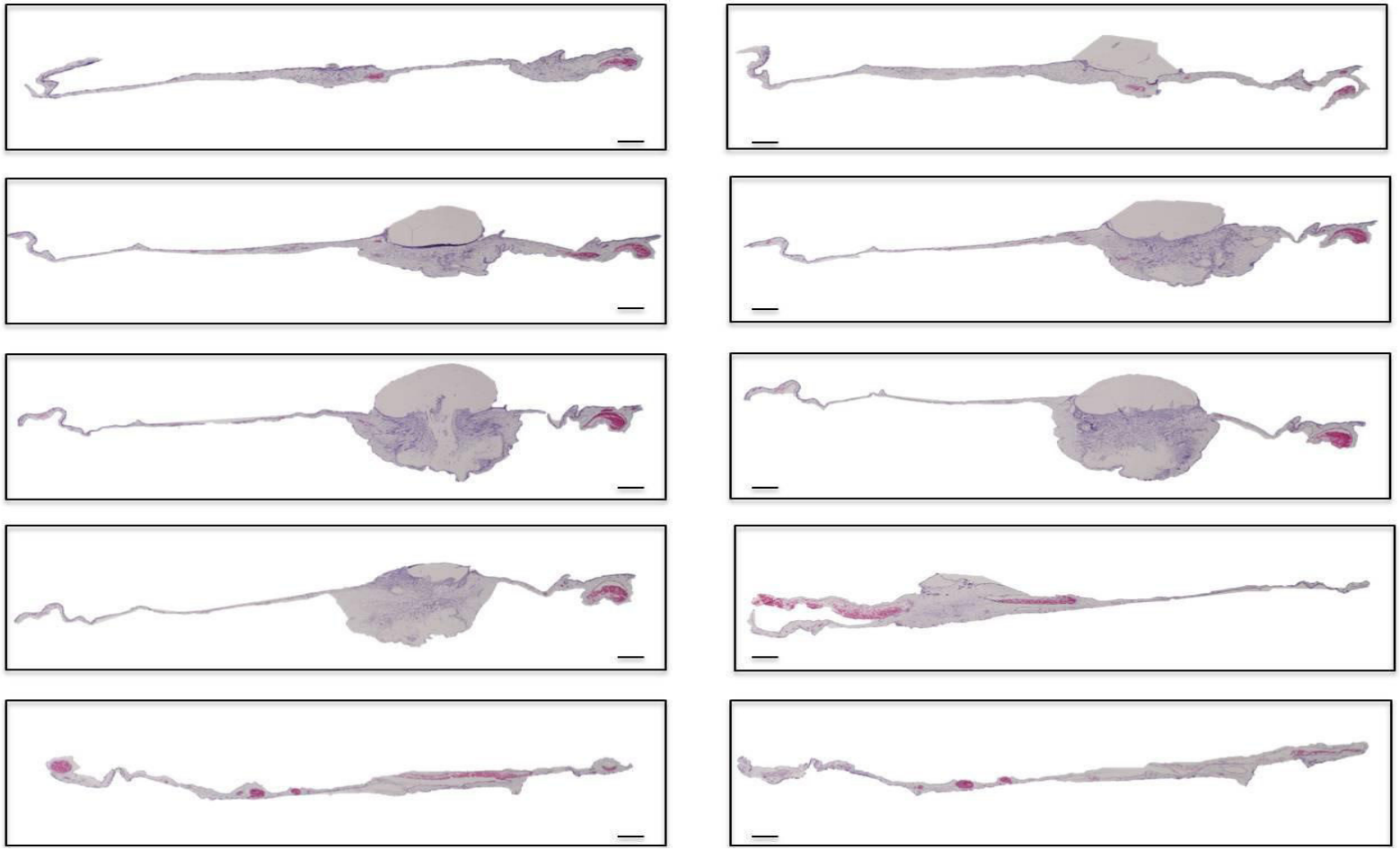

Figure19 Microscopic observation of histological sections through the developed tumour of P-STS spheroids with Matrigel™. After 3 days of tumour development on CAM the accrued xenograft was processed through histological fixation and paraffin embedding. Each 25th 5µm thick section was stained with H/E. Overview through the whole tumour. Bar:200µm

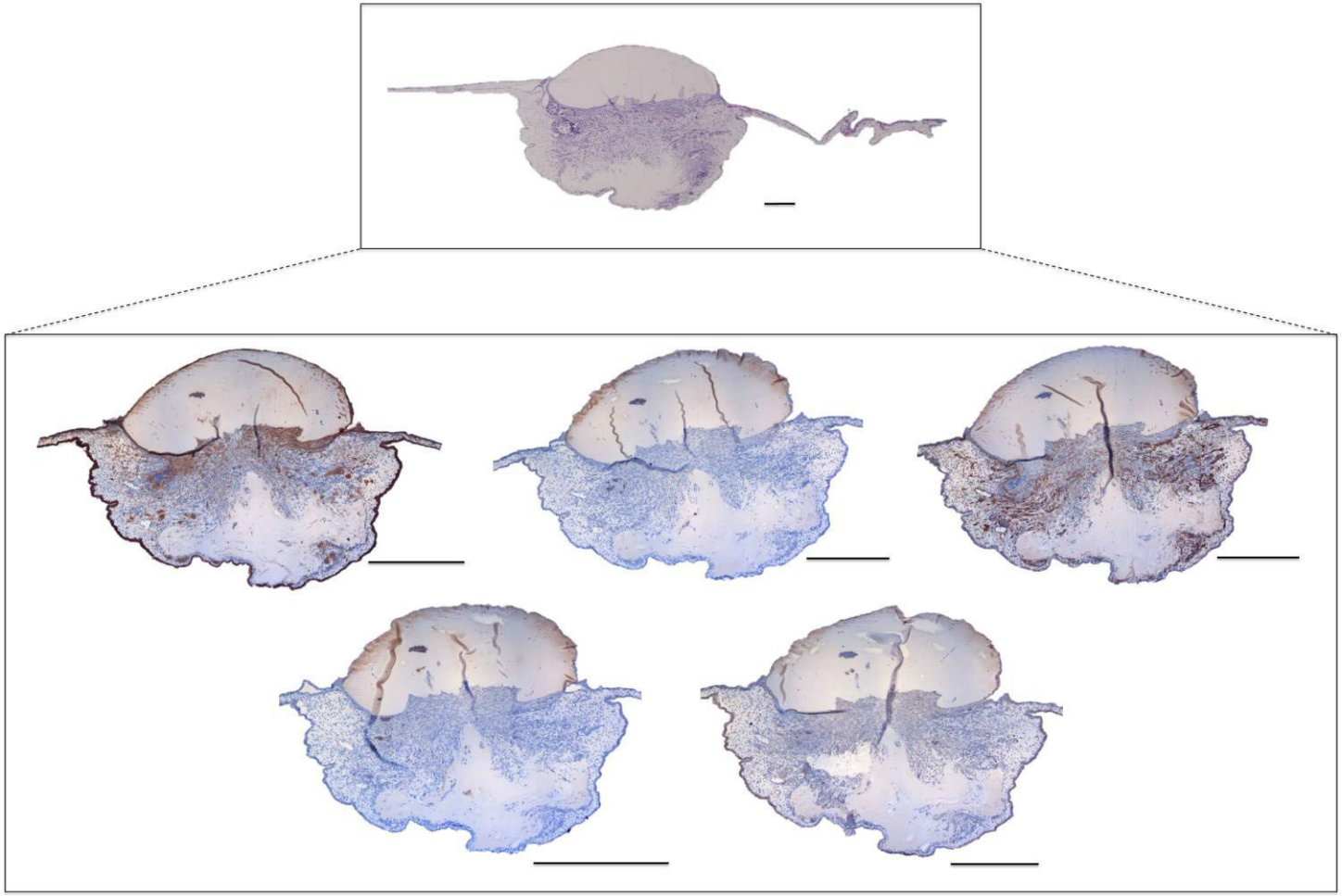

Figure 20 Histological sections of 3 days old tumour xenograft of P-STS spheroid with Matrigel™ stained with SI-NET markers (cytokeratin, synaptophysin, chromogranin), Ki-67 (mitosis marker) and desmin. 3 days after xenografting the developed tumour was processed through histological fixation and embedding procession steps. 5µm thick sections were cut and stained chronologically from top to down: H/E staining, cytokeratin, desmin, Ki-67, synaptophysin and chromogranin . Scale bar:200µm

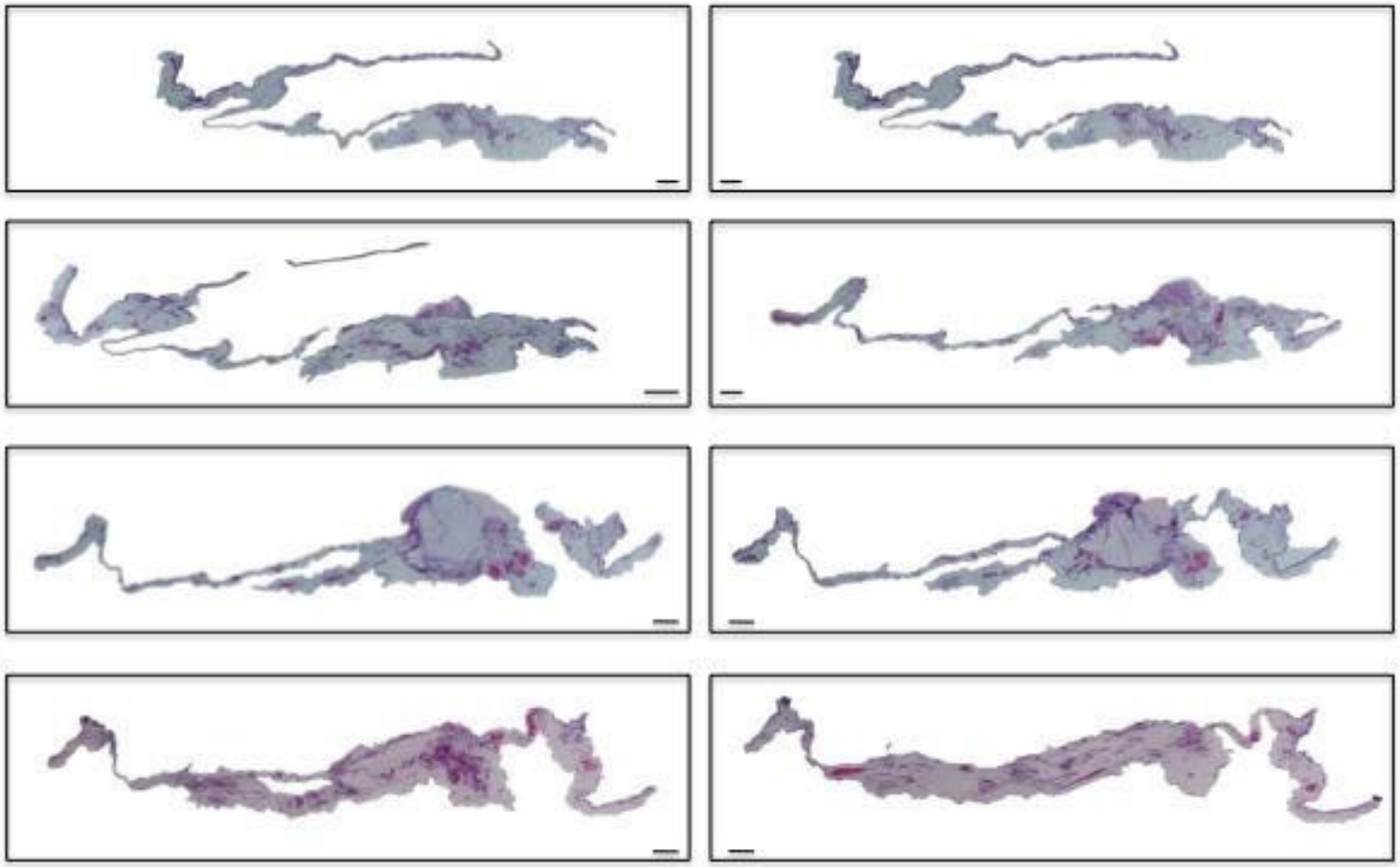

Figure 21 Microscopic observation of histological sections through the developed tumour of single P-STS cells with Matrigel™. After 6 days of tumour development on CAM the accrued xenograft was processed through histological fixation and paraffin embedding. Each 25th 5µm thick section was stained with H/E. Overview through the whole tumour. Bar:200µm

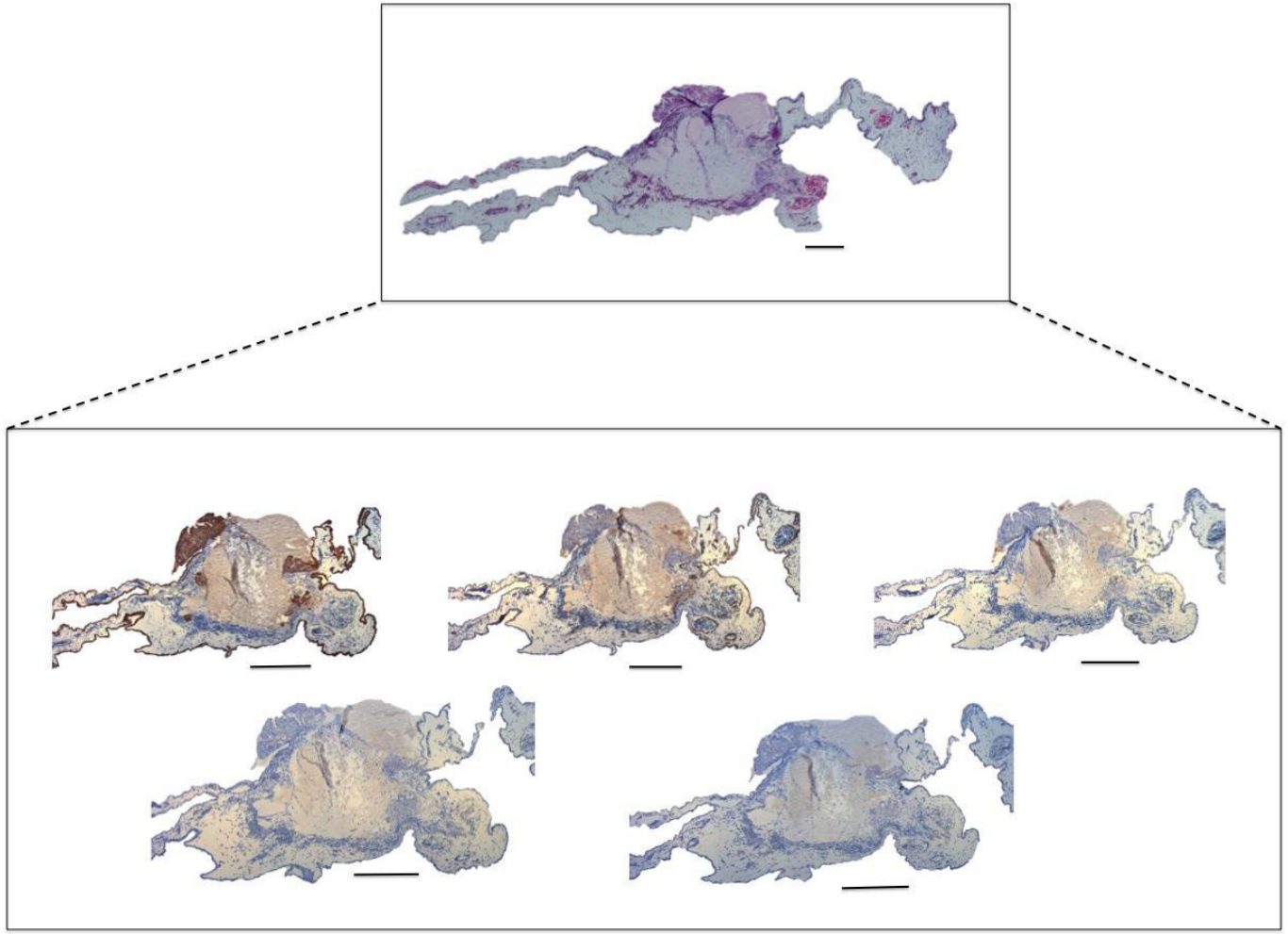

Figure 22 Histological sections of 6 days old tumour xenograft of P-STS single cell with Matrigel™ stained with SI-NET markers (cytokeratin, synaptophysin, chromogranin), Ki-67 (mitosis marker) and desmin. 6 days after xenografting the developed tumour was processed through histological fixation and embedding procession steps. 5µm thick sections were cut and stained chronologically from top to down: H/E staining, cytokeratin, desmin, Ki-67, synaptophysin and chromogranin . Scale bar:200µm

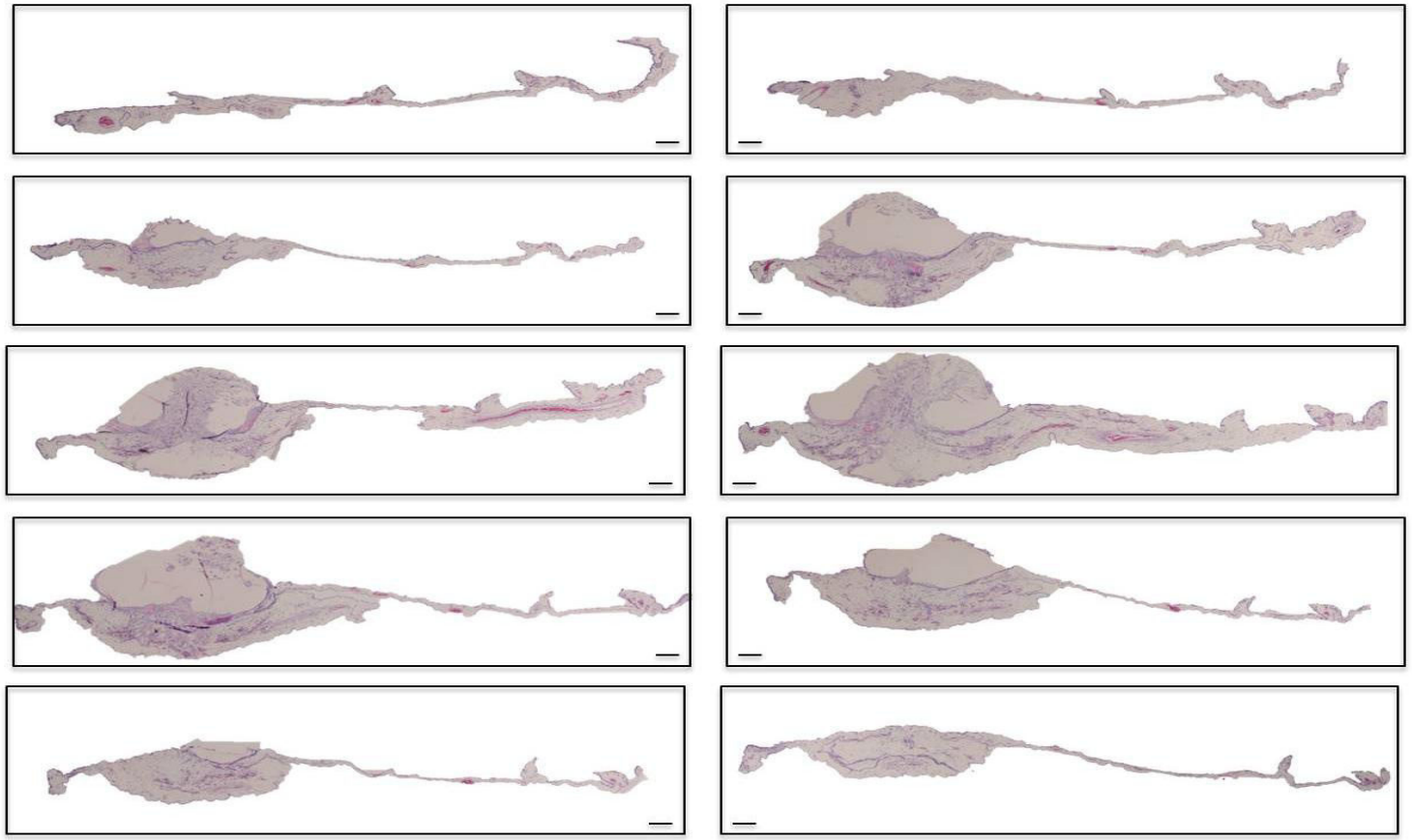

Figure 23 Figure 24 Microscopic observation of histological sections through the developed tumour of P-STS spheroids with Matrigel™. After 6 days of tumour development on CAM the accrued xenograft was processed through histological fixation and paraffin embedding. Each 25th 5µm thick section was stained with H/E. Overview through the whole tumour. Bar:200µm

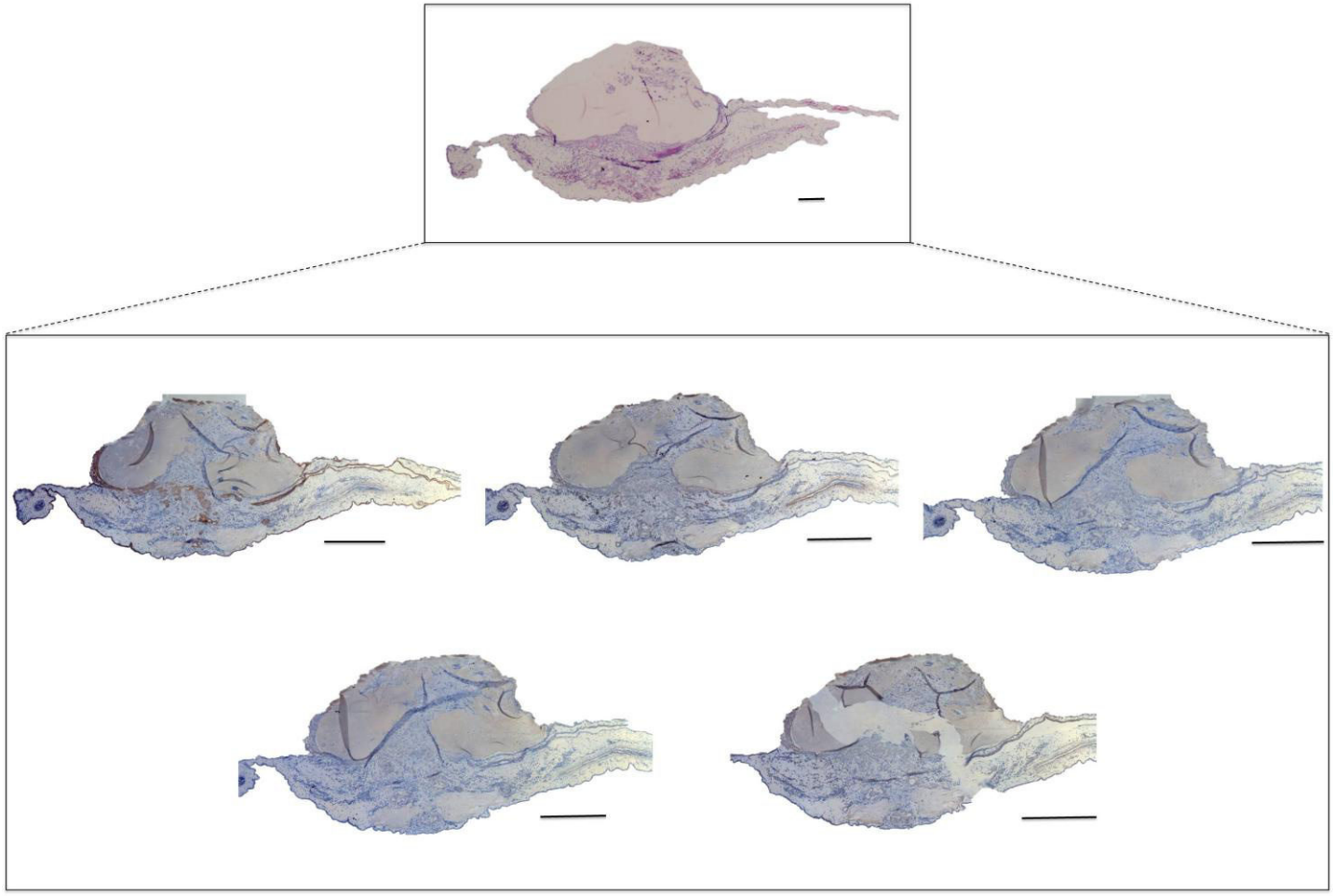

Figure 25 Histological sections of 6 days old tumour xenograft of P-STS spheroid with Matrigel™ stained with SI-NET markers (cytokeratin, synaptophysin, chromogranin), Ki-67 (mitosis marker) and desmin. 6 days after xenografting the developed tumour was processed through histological fixation and embedding procession steps. 5µm thick sections were cut and stained chronologically from top to down: H/E staining, cytokeratin, desmin, Ki-67, synaptophysin and chromogranin . Scale bar:200µm

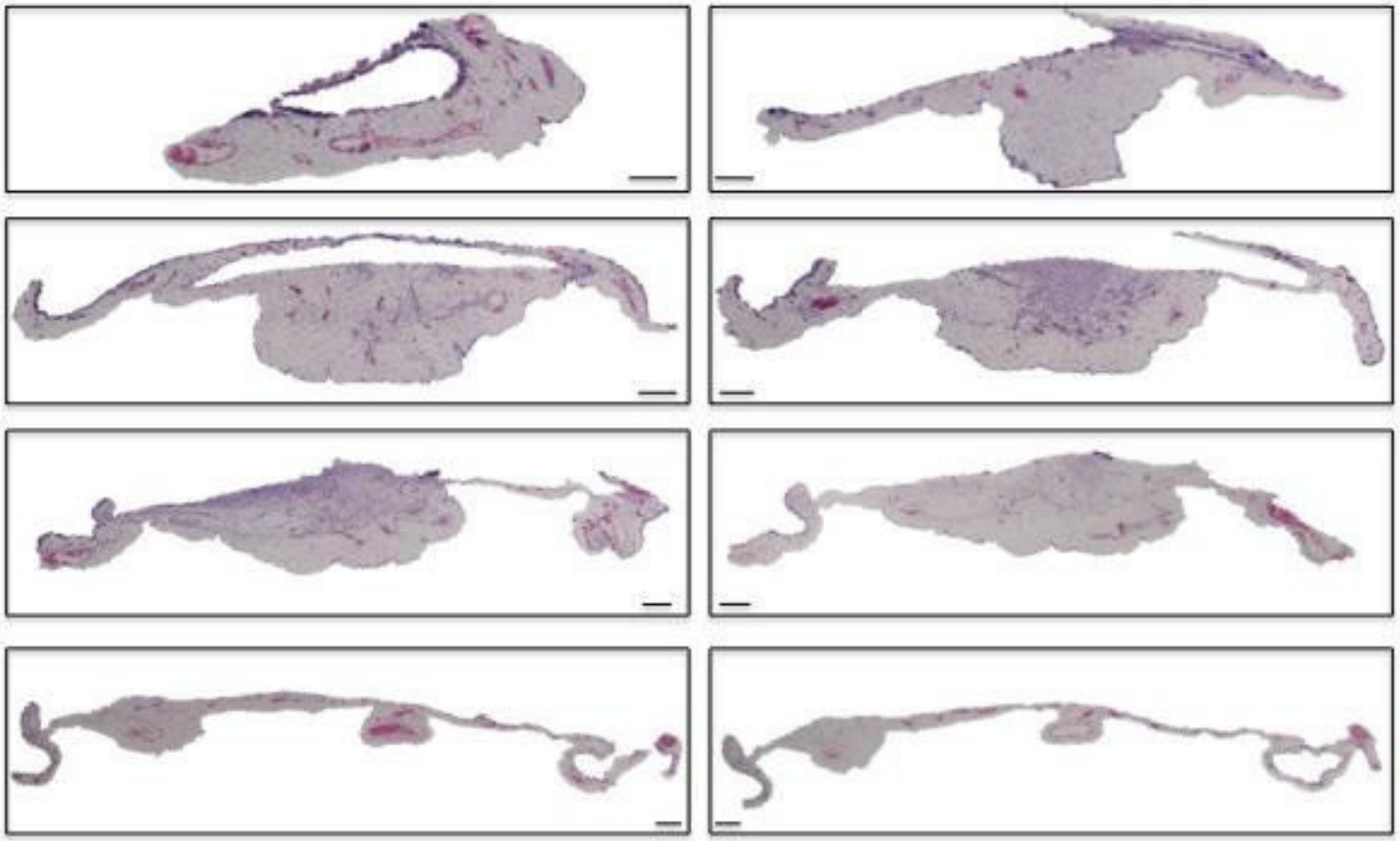

Figure 26 Microscopic observation of histological sections through the developed tumour of single P-STS cells without Matrigel™. After 3 days of tumour development on CAM the accrued xenograft was processed through histological fixation and paraffin embedding. Each 5th 5µm thick section was stained with H/E. Overview through the whole tumour. Bar:200µm

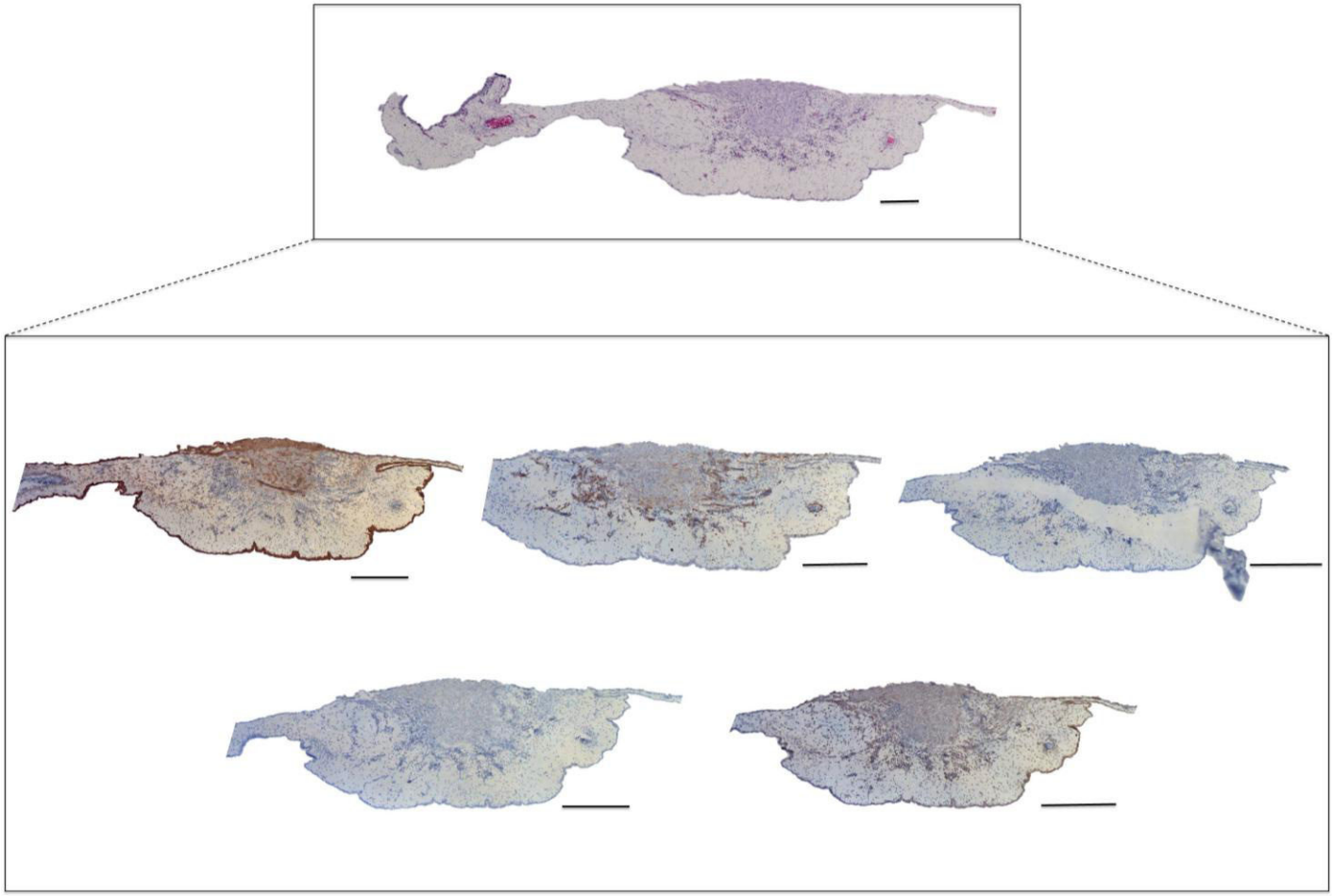

Figure 27 Histological sections of 3 days old tumour xenograft of P-STS single cell without Matrigel™ stained with SI-NET markers (cytokeratin, synaptophysin, chromogranin), Ki-67 (mitosis marker) and desmin. 3 days after xenografting the developed tumour was processed through histological fixation and embedding procession steps. 5µm thick sections were cut and stained chronologically from top to down: H/E staining, cytokeratin, desmin, Ki-67, synaptophysin and chromogranin . Scale bar:200µm

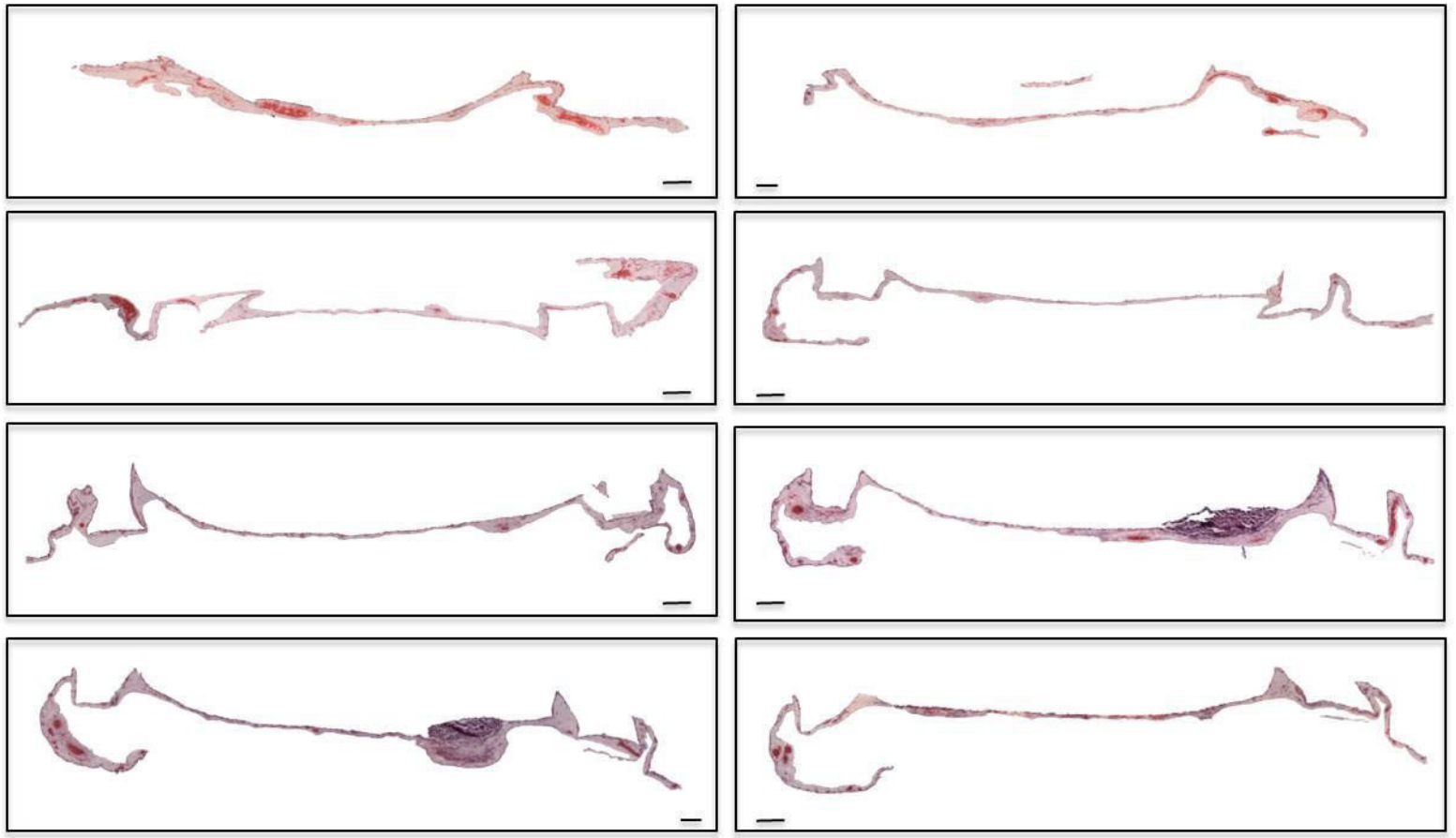

Figure 28 Microscopic observation of histological sections through the developed tumour of P-STS spheroids without Matrigel™. After 3 days of tumour development on CAM the accrued xenograft was processed through histological fixation and paraffin embedding. Each 25th 5µm thick section was stained with H/E. Overview through the whole tumour. Bar:200µm

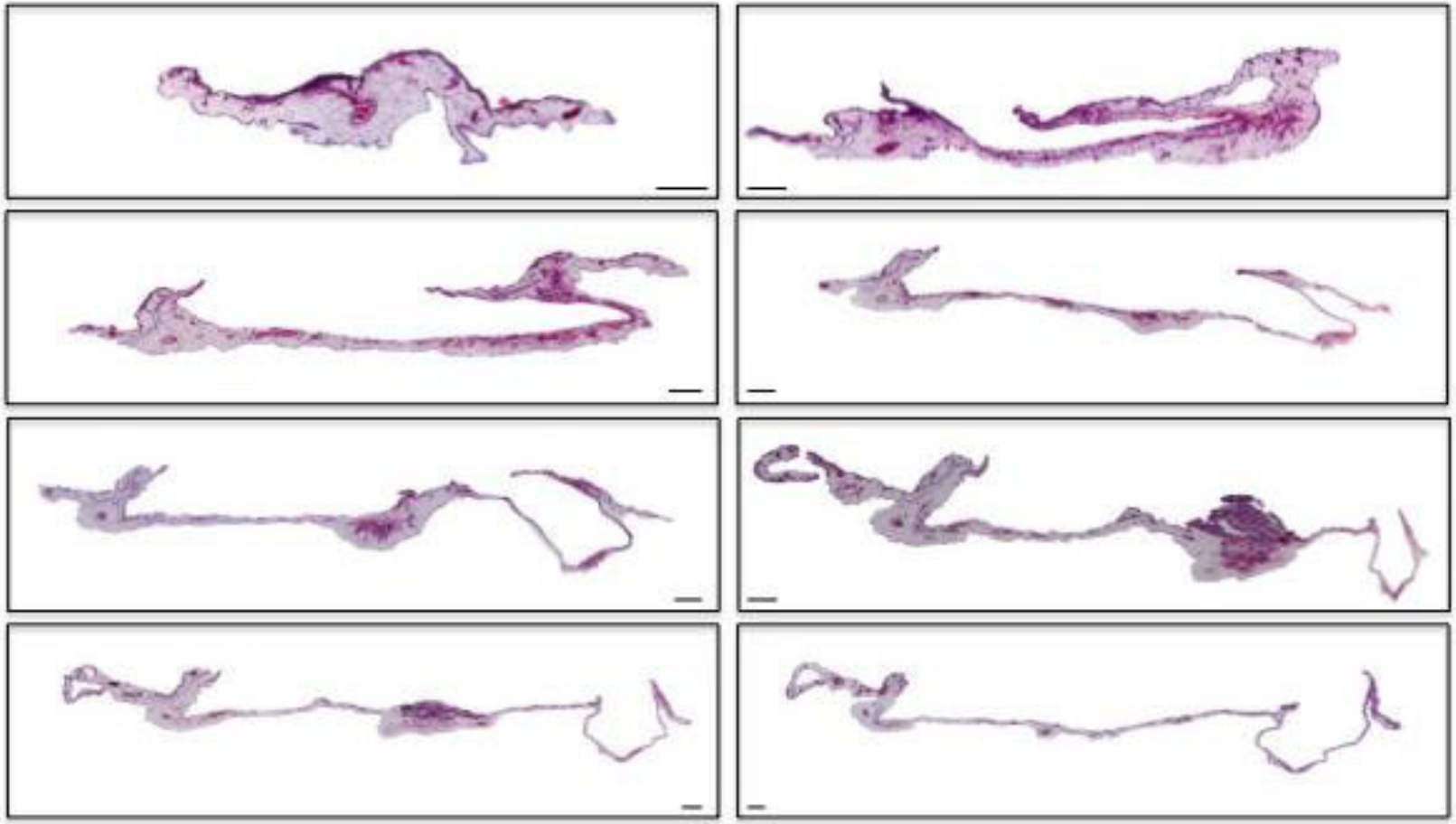

Figure 29 Microscopic observation of histological sections through the developed tumour of P-STS spheroid without Matrigel™. After 6 days of tumour development on CAM the accrued xenograft was processed through histological fixation and paraffin embedding. Each 25th 5µm thick section was stained with H/E. Overview through the whole tumour. Bar:200µm

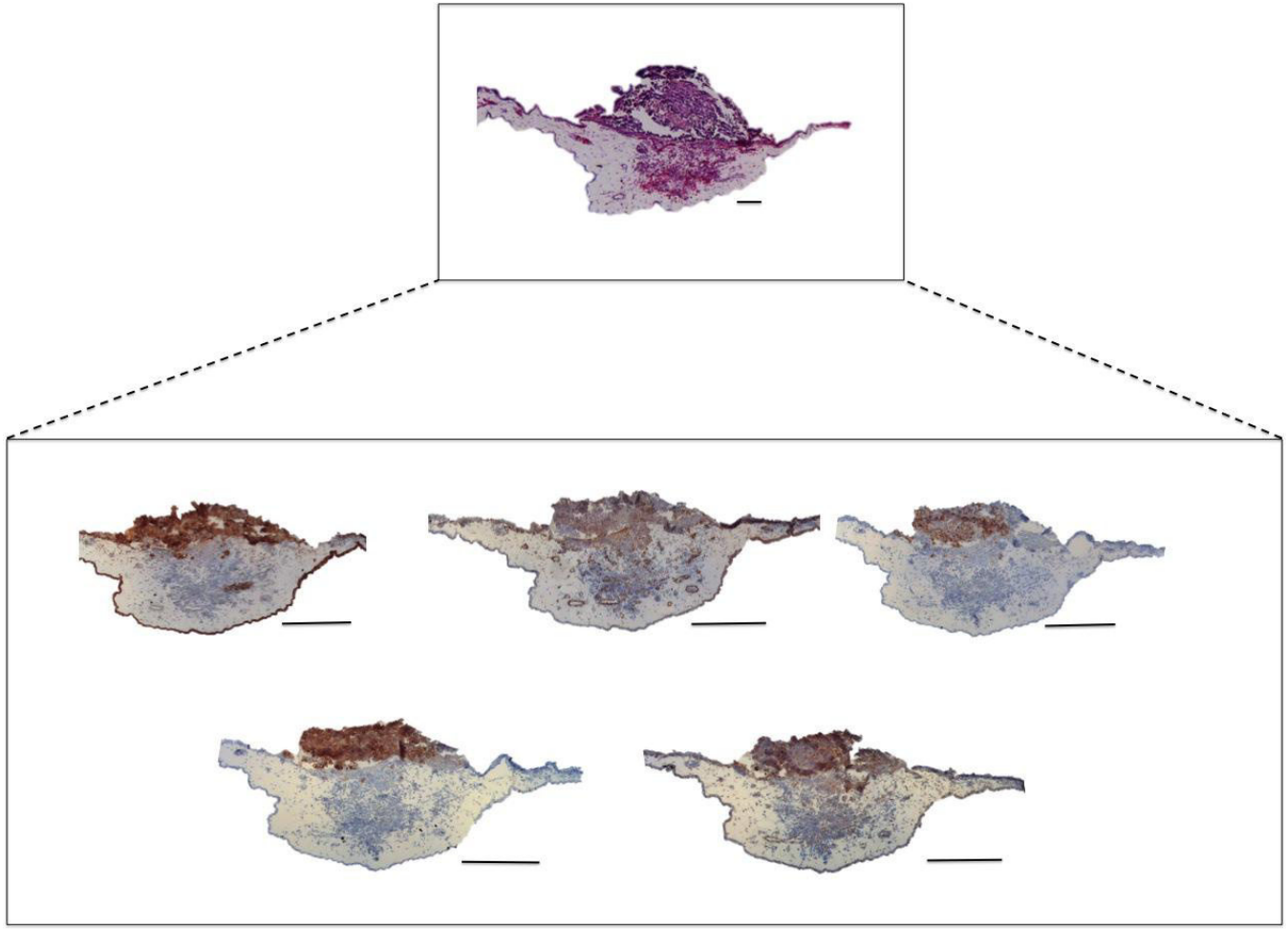

Figure 30 Histological sections of 6 days old tumour xenograft of P-STS spheroids without Matrigel™ stained with SI-NET markers (cytokeratin, synaptophysin, chromogranin), Ki-67 (mitose marker) and desmin. 6 days after xenografting the developed tumour was processed through histological fixation and embedding procession steps. 5µm thick sections were cut and stained chronologically from top to down: H/E staining, cytokeratin, desmin, Ki-67, synaptophysin and chromogranin . Scale bar:200µm

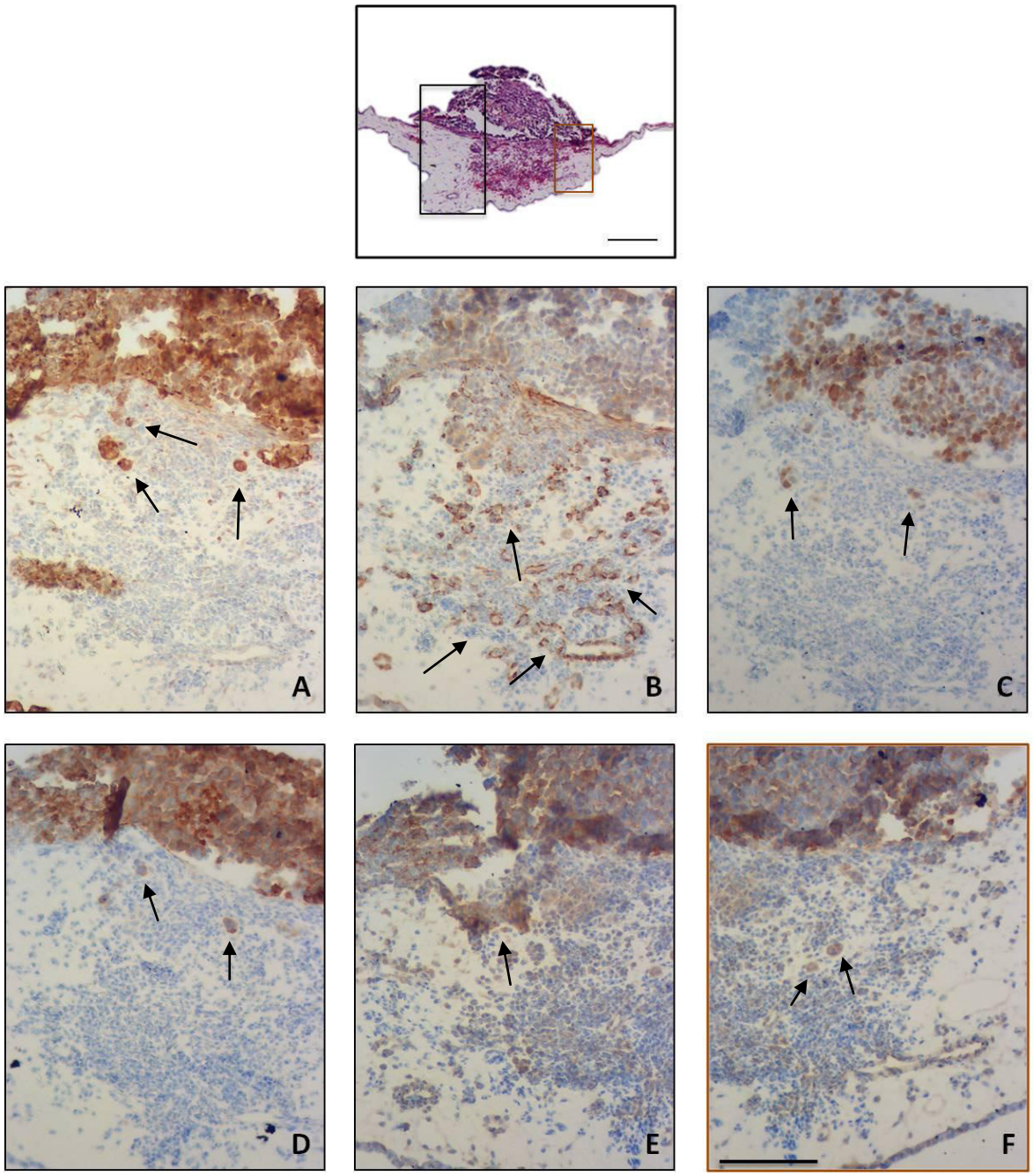

Figure31 Immunhistochemical examination of 6 day old spheroid onplants: Immunhistological staining with A: Cytokeratin, B: Desmin, C: Ki67, D: Synapthophysin, E & F: Chromogranin-A. Arrows in A, C-F indicate invasive P-STS tumour cells. Arrows in B show neovascularisation. Counterstaining haematoxyline. Scale bar: 100µm

4. DISCUSSION

The CSC theory implies that only a small sub-population of cells is responsible for tumourigenesis and establishes the cellular heterogeneity within the primary tumour.[38, 63, 64] Furthermore, CSCs are thought to be capable of self-renewal, differentiation, tumour growth and drug resistance. In recent years the investigation of CSC markers increased in order to aid the development of new and more efficient chemotherapeutics and anti-cancer drugs.[63, 65-67]

In this study, I hypothesise that NETs contain a subpopulation of cells termed neuroendocrine cancer stem cells that are responsible for malignant properties of NET tumours, in particular for cell invasion and the induction of angiogenesis. The conventional first step to identify CSC population in cancer cells is the staining with labelled antibodies against cell surface CSC markers and separation of labelled and unlabelled cells *via* flow cytometry or magnetic columns.[12, 65, 66] The difficulty is that in contrast to other human neoplasms such as breast-, prostate-, colon- or lung cancer, in NETs no specific CSC surface markers could be identified so far, probably due to the rareness of NETs and the difficulties to establish NET cell lines. Gaur *et al.* tried to define a CSC marker for GI-NETs in patient derived probes, their work served as basis for my study.[39]

In my work, I first screened for the most popular stem cell genes and surface markers described in connection with the CSC content in the well-established SI-NET cell line P-STS *via* semi-quantitative RT-PCR. My results revealed that almost all tested surface markers (CD133, CD15, CD117 & CD24) and several other putative stem cell related genes (Nestin; MSI1; BMI1; ID-1; OCT4; Nanog) are present in detectable amounts in the P-STS cell line. Even though ALDH expression was not found in the P-STS cells at RNA level, the ALDH activity assay *via* FACS analysis was examined. In concordance to results from Gaur and collegues, 2.5% of P-STS cells show $ALDH^+$ activity. Gaur *et al.* suggested that the $ALDH^+$ population has the potential to be a CSC marker for GI-NETs.[39] Enzymes of the ALDH superfamily have various functions and are involved in detoxification processes, production of antioxidants as well as synthesis of neurotransmitters (e.g. retinoic acid and *gamma*-Aminobutyric acid), which both are accountable for

supply and differentiation of normal and cancer stem cells.[65, 68] ALDH, said to be a hallmark of cancer stem cells, is one of the most measured factors correlated to CSC markers and was detected in almost every known type of cancer, such as breast cancer[37], colon cancer[50], head and neck squamous cell carcinoma[69, 70], pancreatic carcinoma[71], lung cancer[72] and prostate cancer[64]. There have been conflicting reports whether a small or a rather large population of cells with $ALDH^{high}$ activity are better indicators of CSC cells.[39, 53] Basically, ALDH is often used in conjunction with other CD markers to identify a distinct CSC population. [73] However, there is evidence that a high ALDH activity is related to poor prognoses and survival rates in breast and prostate cancer.[37, 52] Moreover, an increased ALDH activity showed a correlative connection to high tumourigenesis, to an enhanced stem cell characteristic (*in vivo* and *in vitro*) and also to a poor cure in malignant melanomas.[74] One of the first attempts was to use known ALHD properties for therapy of leukemia patients with all-trans retinoic acid (ATRA) treatment. The clinical impact of ALDH was shown by Moreb *et al.*, who treated leukemia patients with all-trans retinoic acid (ATRA), forcing the down-regulation of ALDH activity: Nowadays, a combination of chemotherapy and ATRA is part of classical therapy treatment to cure acute promyelocytic leukemia.[65, 67, 75, 76]

In my research I analysed 4 of the most common CD markers described in the literature, e.g. CD133, CD24, CD44, and CD117.

The most- prominent CD marker in the context of CSC is CD133 (also known as "Prominin"). The membrane glycoprotein CD133 was first detected as a hematopoietic stem cell marker.[32] Numerous publications followed to demonstrate the versatile properties of CD133 as CSC marker. For example, glioblastoma and colorectal carcinoma both express CD133, but only the $CD133^{+}$ subsets turned out to be high tumorigenic and exhibited the ability to cause heterogeneity. The P-STS cell line had a very high expression (98%) of CD133, which leads me to the conclusion that CD133 cannot act as a CSC marker in this cell line. In contrast to my data, Gaur *et al.*, were not able to measure any CD133 expressions.[39]

The combination of CD24/CD44 surface markers is used to isolate breast cancer stem cells with tumourigenic potential.[77] In addition, CD44 is also a CSC population marker for gastric cancer. Takaishi isolated CD44 subpopulation in

gastric cancer that showed self-renewal and differentiation capacities. [33] In my study, the P-STS cell line showed no CD 44 expression, however, 43.9% of the cells were CD24 positive. Due to the high CD 44 and CD 24 expression level it is not possible to identify a CSC subpopulation; the percentage is higher than 5% therefore not fulfill the criteria for being CSCs.

The receptor tyrosine kinase CD117 is a well-known oncogene and is shown by several groups to be expressed on stem cells. Luo *et al.* determined the characteristics of CSC in a sorted $CD117^+$ lineage ovarian cancer population. Moreover, they observed that $CD117^+$ patients are less sensitive to chemotherapy than $CD117^-$.[55] In comparison to ovarian cancer, P-STS cells have a very high number of CD117 expressing cells (48% of total), suppositious that only a small population of tumour cells bears stem cell properties, and this high percentage of cell number appears to be too high.

Recent studies showed an increase of self-renewal capacity and enhanced CSC marker expression in spheroids compared to conventional 2D monolayer cultivation. [31, 78] Expression of the self-renewal genes confirmed *via RT-PCR and* the spheroid formation attested the presence of CSC subpopulation in P-STS cell line. To evaluate differences of CSC related stem cell genes and surface markers expression in 2D *vs.* 3D, quantitative RT PCR was performed. Moderate increase of CD117 and CD24, but a lower CD133 expression in spheroid cultures was already observed by Fujiwara *et al.*; oesophageal squamous cell carcinoma showed also a weaker CD133 expression in spheroids.[70] However, Qiu *et al.* and He *et al.* reported the increase of the capacity of self-renewal-, detoxification- and expression surface markers in 3D compared to 2D cultures of ovarian and lung cancer.[20, 23]

The mRNA quantity of almost all stem cell related genes has changed in P-STS cell line following 3D cultivation. While BMI1 expression remains almost unchanged, SOX2, Nanog, Nestin, MSI-1, ID-1, CD24 and CD117 exhibited an increased expression, a reduction of mRNA amounts was found for Oct4, ABCG2 and CD133.

BMI1 (B-cell-specific Moloney murine leukemia virus insertion site 1), a part of the polycomb repressive complex 1, plays an important role in self-renewal and proliferation of stem cells by modifying histones via methylation and thus altering the chromatin structure.[79] The cooperation of BMI-1 with c-Myc protein forms a stable transcriptional repressor, which *via* INK4a/ARF negatively regulates the transcription of $p16^{Ink4a}$ and $p19^{Arf}$.[60, 79] Apart from the proliferative function in hematopoietic, neural and mammary stem cells, BMI-1 is up-regulated in various cancer types such as breast[80], colorectal[81] and prostate cancer[60] and oral squamous cell carcinoma[79]. Chen *et al.* showed that knockdown of the endogenous BMI-1 in primary laryngeal tumours supports apoptosis and represses proliferation. They also described a correlation between expression level and differentiation status of the tumour cells; high differentiated tumour cells evidenced a stronger expression of BMI-1 than the lower once.[79] Furthermore, results published by Song *et al.* confirm the decline of proliferation and growth in pancreatic cancer cells as well as tumourigenicity in an *in vitro* model.[82] Kim *et al.* observed a higher expression BMI-1 in breast carcinomas compared to normal breast tissue. Additionally, they assumed that the extent of BMI-1 expression correlates with invasion and progression properties of breast cancer.[80] In P-STS, BMI1 was highly expressed, but expression remained almost unchanged following 3D cultivation. Therefore my results do not correspond with data published in the literature for other cancer types.

Nestin and Musashi are both proteins expressed in neural progenitor cells during central neural system development and down-regulated in mature cells and adult tissue. Nestin is an intermediate filament protein first discovered in neuroepithelial stem cells involved in the organisation of the cytoskeleton, cell signalling, organogenesis and cell metabolism.[59, 83] Strojnik *et al.* proposed, consistent with a publication of Florenes *et al.* that an increase of Nestin correlates with invasiveness and malignancy of glioblastomas.[59, 84] Therefore, Nestin could be a strong prognostic marker. Furthermore, it is not surprising that an enhanced Nestin expression is also correlated with a poor outcome of gliomas.

Musashi, an RNA-binding protein, was first described in neural stem cells and is responsible for translational regulations of differentiation, tumourigenesis and

control of early asymmetric division.[59, 85, 86] It turned out that Nestin is a more independent and stronger marker for glioblastomas than musashi.[59] However, a considerable overexpression was observed in lung cancer[85], intestinal adenomas[87] and hepatomas[88]. Wang *et.al.* identified musahi-1 as an independent risk factor of lung cancer.[85] In my study both, Nestin and Musashi expressions were significantly increased in 3D cultured cell than in 2D (Figure 12).

In recent reports ID-1(DNA-binding protein inhibitor) is described as a key mediator of cell growth, differentiation and tumourigenesis.[89] Other studies claim the regulative role of ID-1 in cell cycle progression by promoting G1/S transitions.[90, 91] ID-1 is one of four ID family members, which belong to the helix-turn-helix (HLH) proteins. This protein family acts as an antagonist of the basic helix-turn-helix (bHLH) proteins, which are transcription factors (TF) responsible for development, proliferation and differentiation of cells.[89, 90, 92] ID proteins are capable of dimerizing with bHLH, thus preventing the binding to DNA.[93] The most interesting and investigated family member is ID-1 because of its up-regulated expression level in several tumours and cancer cell lines: gastric cancer[89], mouse embryonic carcinoma PL19CL6 cells[90], lung carcinoma[92] and non-small cell lung carcinoma[94], human oral squamous cell carcinoma cells[93], endometrial carcinoma[91], colon carcinoma[89] and lymph node metastasis.[93] I also detected an enhanced overexpression in P-STS spheroids, which might constitute an increased tumour growth and cell proliferation promoted by ID-1.[90] Rothschild *et al.* and Han *et al.* examined an ID-1 presence and up-regulation in an early stage of non-small cell lung cancer as well as gastric cancer and suggested the use of an ID-1 marker for detection.[89, 94] Furthermore, a knockdown of ID-1 reduced the proliferation and invasiveness of squamous cell carcinoma.

The three most important determined stem cell related genes, which are accountable for self-renewal and pluripotency of embryonic stem cells, are the core transcription factors Sox2, Oct4 and Nanog. Both, Sox2 and Oct4 are overexpressed in various cancers and are able to reprogram differentiated cells into pluripotent cells in connection with other factors. [95, 96] Rodda *et al.* described the cooperative linkage between Sox2 and Oct4 with the Nanog proximal promoter. Chiou et al showed that the overexpression of Nanog and Oct4 in lung

adenocarcinoma lead to enhanced number of CD133+, cells supports spheroid formation and enhances treatment resistance. It is also described that Nanog expression is depending on the regulation of its upstream target Oct4. [56] In the P-STS cell line a massive enhancement of Nanog and Sox2 expression in 3D spheroids was detected, conversely the Oct 4 expression was higher in 2D cultivated P-STS. In sum, all three genes are present in spheroids, even thought SOX2 and Nanog are upregulated in comparsion to Oct4. Because of the bearing of Oct4 to Nanog and Sox2 to Nanog, the gene expression leads to the conclusion, that Sox2 has a greater impact on regulation of Nanog expression than Oct4.

The discovered changes in gene expression gave rise to the question whether 3D cultivated P-STS cells have more invasive growth behaviour *in vivo*.

In general, the method of choice to examine tumourigenesis of malignant cells is xenotransplantation in immunodeficient mice. In my research I used an alternative method, the CAM assay, to investigate tumourigenesis and invasion of 2D and 3D cultivated P-STS cells over a period of 6 days. In comparison to mouse experiments, the CAM assay has several advantages: the easy handling and the good accessibility of the membrane allows a quick experimental setup In addition it is cost effective, reproducible and, one of the most important advantages is that according to European community guidelines for animal experiments, it counts as an alternative method. To facilitate the invasion, cells were mixed with Matrigel™. All experiments, performed with Matrigel™, resulted in formation of dense, round shaped tumours, comparable to a pinhead, with an approximate diameter of at least 200 µm. In this context Matrigel™ with its growth factors operates as starting aid for the cells. However, the histological sections of 3 days and 6 days old xenografts showed considerable disadvantage of Matrigel™. The amount of Matrigel™, with a ratio of 1:2, which was used in the experiments, was definitely too high, leading to massive overloading of the thin chorioallantoic membrane and eventually Matrigel™ breaks through the CAM epithelium into the stromal tissue. Moreover the omnipresence of Matrigel™ in the sections causes the non-specific binding of antibody during immunohistochemistry staining and leads to undesirable results.

All together, I performed 63 CAM assays using 15.000 2D or 3D cultivated P-STS cells mixed with Matrigel™, see supplementary table 13.

Only 3 out of 16 onplants of 2D cultivated P-STS cells without Matrigel™ developed small tumours on the CAM, 7 were not able to generate a distinct tumour and formed streaks, and 6 even showed no tumour incurrence, indicating the importance of the growth factors in Matrigel™ for the tumour initiation.

In contrast, 25 prominent tumours have developed out of the 3D cultivated P-STS cells on the CAM. However, 8 of 36 spheroids transplanted without Matrigel™, showed streaks instead of forming compact tumours on the CAM surface and 3 experiments revolved no tumour.

The comparison of 2D *vs* 3D tumour formation without Matrigel™ points out, that 3D spheroids have more capacity for tumour formation than cells as monolayer. The immunohistological staining confirmed the more invasive behaviour of tumour spheroids. Figure31 shows a detailed view of 6 days grafted spheroids without Matrigel™. The staining indicates the invasion through the CAM (shown in Figure31 A, D and E by arrows). The desmin staining demonstrated an immense accumulation of micro blood vessels (arrows Figure31 B), precisely where inflammatory reaction was suspected (Figure 29, arrows). The tumour spheroid was stained positive for the mitotic factor Ki-67, indicating high mitogenic activity of the P-STS cells.

Even though single cells cover the whole (silicone ring) CAM surface and assumed to have the ability to act more invasive, 69% of spheroids generated tumours, whereas only 18% of the monolayer onplants were able to form distinct tumours. Expanding the time period of grafting from 3 to 7 days showed no beneficial effect of tumour growth in spheroids without Matrigel™. Contrary, this longer cultivation time of single cell grafts demonstrated a decline of tumour initiation and growth. Based on my findings it can be assumed that the increased invasive behaviour of spheroids is attributable to changed cell properties. The latter activates other genes, which promote the enhanced invasiveness of the tumours and most likely correlates with CSC related genes. To confirm this statement, a detailed study of each CSC related gene appears reasonable. One

approach would be to over-express the CSC related gene of interest in P-STS cells and survey weather this affect the invasion. The down-regulation of the same gene could cause the opposite outcome. Furthermore, specific stimulators and Inhibitors could be administered to elucidate the pathophysiology of the mechanisms underlying the tumourigenic behaviour of P-STS cells. Together, the resulted data could pave the way towards more efficient treatment of NET, but also of other malignancies.

Conclusion:

In my work I provided the evidence that the P-STS cell line showed various characteristics of a CSC subpopulation:

- CSC related genes are expressed in P-STS cell line,
- P-STS cells are able to form spheroids,
- The expression of CSC related genes are changed in spheroids–most genes are overexpressed,
- ALDH activity is found in a promising subpopulation of 2.5%,
- grafted spheroids demonstrate a more invasive behaviour than single cells

5. REFERENCES

1. DeLellis RA. The neuroendocrine system and its tumors: An overview. Am J Clin Pathol. 2001 Jun;115 Suppl:S5-16.

2. Modlin IM, Oberg K, Chung DC, Jensen RT, de Herder WW, Thakker RV, Caplin M, Delle Fave G, Kaltsas GA, Krenning EP, Moss SF, Nilsson O, Rindi G, Salazar R, Ruszniewski P, Sundin A. Gastroenteropancreatic neuroendocrine tumours. Lancet Oncol. 2008 Jan;9(1):61-72.

3. Hauso O, Gustafsson BI, Kidd M, Waldum HL, Drozdov I, Chan AK, Modlin IM. Neuroendocrine tumor epidemiology: Contrasting norway and north america. Cancer. 2008 Nov 15;113(10):2655-64.

4. Strosberg J. Neuroendocrine tumours of the small intestine. Best Pract Res Clin Gastroenterol. 2012 Dec;26(6):755-73.

5. Adam M. Mougey, MD, and Douglas G. Adler, MD. Neuroendocrine tumors: Review and clinical update. Hospital Physician. 2007;43:12-51.

6. Pfragner R, Behmel A, Hoger H, Beham A, Ingolic E, Stelzer I, Svejda B, Moser VA, Obenauf AC, Siegl V, Haas O, Niederle B. Establishment and characterization of three novel cell lines - P-STS, L-STS, H-STS - derived from a human metastatic midgut carcinoid. Anticancer Res. 2009 Jun;29(6):1951-61.

7. Oberg K. Diagnostic pathways In: Martyn Evan Caplin, Larry Kvols, editor. Handbook of neuroendocrine tumours. Their current and future management. Bioscientifica; p. 103-19.

8. Modlin IM, Shapiro MD, Kidd M. Siegfried oberndorfer: Origins and perspectives of carcinoid tumors. Hum Pathol. 2004 12;35(12):1440-51.

9. Christopoulos EP,C. Gastric neuroendocrine tumors: Biology and management. Annals of Gastroenterology. 2005;18(2)

10. WILLIAMS ED, SANDLER M. The classification of carcinoid tum ours. Lancet. 1963 Feb 2;1(7275):238-9.

11. Reynolds I, Healy P, Mcnamara DA. Malignant tumours of the small intestine. The Surgeon. 2014 10;12(5):263-70.

12. Guo W, Lasky JL, Wu H. Cancer stem cells. Pediatr Res. 2006 print;59:59R-64R.

13. BRUCE WR, VAN DG. A quantitative assay for the number of murine lymphoma cells capable of proliferation in vivo. Nature. 1963 07/06;199(4888):79-80.

14. Bonnet D, Dick JE. Human acute myeloid leukemia is organized as a hierarchy that originates from a primitive hematopoietic cell. Nat Med. 1997 Jul;3(7):730-7.

15. Al-Hajj M, Wicha MS, Benito-Hernandez A, Morrison SJ, Clarke MF. Prospective identification of tumorigenic breast cancer cells. Proceedings of the National Academy of Sciences. 2003 April 01;100(7):3983-8.

16. Singh SK, Clarke ID, Terasaki M, Bonn VE, Hawkins C, Squire J, Dirks PB. Identification of a cancer stem cell in human brain tumors. Cancer Res. 2003 Sep 15;63(18):5821-8.

17. Fang D, Nguyen TK, Leishear K, Finko R, Kulp AN, Hotz S, Van Belle PA, Xu X, Elder DE, Herlyn M. A tumorigenic subpopulation with stem cell properties in melanomas. Cancer Res. 2005 Oct 15;65(20):9328-37.

18. Tirino V, Desiderio V, Paino F, De Rosa A, Papaccio F, Fazioli F, Pirozzi G, Papaccio G. Human primary bone sarcomas contain CD133+ cancer stem cells displaying high tumorigenicity in vivo. FASEB J. 2011 Jun;25(6):2022-30.

19. Harma V, Virtanen J, Makela R, Happonen A, Mpindi JP, Knuuttila M, Kohonen P, Lotjonen J, Kallioniemi O, Nees M. A comprehensive panel of three-dimensional models for studies of prostate cancer growth, invasion and drug responses. PLoS One. 2010 May 3;5(5):e10431.

20. He QZ, Luo XZ, Wang K, Zhou Q, Ao H, Yang Y, Li SX, Li Y, Zhu HT, Duan T. Isolation and characterization of cancer stem cells from high-grade serous ovarian carcinomas. Cell Physiol Biochem. 2014;33(1):173-84.

21. Chan KS, Espinosa I, Chao M, Wong D, Ailles L, Diehn M, Gill H, Presti J, Chang HY, van de Rijn M, Shortliffe L, Weissman IL. Identification, molecular characterization, clinical prognosis, and therapeutic targeting of human bladder tumor-initiating cells. Proceedings of the National Academy of Sciences. 2009 August 18;106(33):14016-21.

22. Ricci-Vitiani L, Lombardi DG, Pilozzi E, Biffoni M, Todaro M, Peschle C, De Maria R. Identification and expansion of human colon-cancer-initiating cells. Nature. 2007 01/04;445(7123):111-5.

23. Qiu X, Wang Z, Li Y, Miao Y, Ren Y, Luan Y. Characterization of sphere-forming cells with stem-like properties from the small cell lung cancer cell line H446. Cancer Lett. 2012 Oct 28;323(2):161-70.

24. Reya T, Morrison SJ, Clarke MF, Weissman IL. Stem cells, cancer, and cancer stem cells. Nature. 2001 11/01;414(6859):105-11.

25. Gottschling S, Schnabel PA, Herth FJ, Herpel E. Are we missing the target? cancer stem cells and drug resistance in non-small cell lung cancer. Cancer Genomics Proteomics. 2012 Sep-Oct;9(5):275-86.

26. Anderson K, Lutz C, van Delft FW, Bateman CM, Guo Y, Colman SM, Kempski H, Moorman AV, Titley I, Swansbury J, Kearney L, Enver T, Greaves M. Genetic variegation of clonal architecture and propagating cells in leukaemia. Nature. 2011 01/20;469(7330):356-61.

27. Chen K, Huang Y, Chen J. Understanding and targeting cancer stem cells: Therapeutic implications and challenges. Acta Pharmacol Sin. 2013 print;34(6):732-40.

28. Notta F, Mullighan CG, Wang JC, Poeppl A, Doulatov S, Phillips LA, Ma J, Minden MD, Downing JR, Dick JE. Evolution of human BCR-ABL1 lymphoblastic leukaemia-initiating cells. Nature. 2011 Jan 20;469(7330):362-7.

29. Zimmerer RM, Korn P, Demougin P, Kampmann A, Kokemuller H, Eckardt AM, Gellrich NC, Tavassol F. Functional features of cancer stem cells in melanoma cell lines. Cancer Cell Int. 2013 Aug 6;13(1):78,2867-13-78.

30. Chu P, Clanton DJ, Snipas TS, Lee J, Mitchell E, Nguyen ML, Hare E, Peach RJ. Characterization of a subpopulation of colon cancer cells with stem cell-like properties. Int J Cancer. 2009 Mar 15;124(6):1312-21.

31. Wang S, Huang S, Zhao X, Zhang Q, Wu M, Sun F, Han G, Wu D. Enrichment of prostate cancer stem cells from primary prostate cancer cultures of biopsy samples. Int J Clin Exp Pathol. 2013 Dec 15;7(1):184-93.

32. Burgos-Ojeda D, Rueda BR, Buckanovich RJ. Ovarian cancer stem cell markers: Prognostic and therapeutic implications. Cancer Lett. 2012 9/1;322(1):1-7.

33. Takaishi S, Okumura T, Tu S, Wang SS, Shibata W, Vigneshwaran R, Gordon SA, Shimada Y, Wang TC. Identification of gastric cancer stem cells using the cell surface marker CD44. Stem Cells. 2009 May;27(5):1006-20.

34. Prince ME, Sivanandan R, Kaczorowski A, Wolf GT, Kaplan MJ, Dalerba P, Weissman IL, Clarke MF, Ailles LE. Identification of a subpopulation of cells with cancer stem cell properties in head and neck squamous cell carcinoma. Proceedings of the National Academy of Sciences. 2007 January 16;104(3):973-8.

35. Bleau AM, Huse JT, Holland EC. The ABCG2 resistance network of glioblastoma. Cell Cycle. 2009 Sep 15;8(18):2936-44.

36. Ohi Y, Umekita Y, Yoshioka T, Souda M, Rai Y, Sagara Y, Sagara Y, Sagara Y, Tanimoto A. Aldehyde dehydrogenase 1 expression predicts poor prognosis in triple-negative breast cancer. Histopathology. 2011 Oct;59(4):776-80.

37. Ginestier C, Hur MH, Charafe-Jauffret E, Monville F, Dutcher J, Brown M, Jacquemier J, Viens P, Kleer CG, Liu S, Schott A, Hayes D, Birnbaum D, Wicha MS, Dontu G. ALDH1 is a marker of normal and malignant human mammary stem cells and a predictor of poor clinical outcome. Cell Stem Cell. 2007 Nov;1(5):555-67.

38. Tirino V, Desiderio V, Paino F, De Rosa A, Papaccio F, La Noce M, Laino L, De Francesco F, Papaccio G. Cancer stem cells in solid tumors: An overview and new approaches for their isolation and characterization. FASEB J. 2013 Jan;27(1):13-24.

39. Gaur P, Sceusi EL, Samuel S, Xia L, Fan F, Zhou Y, Lu J, Tozzi F, Lopez-Berestein G, Vivas-Mejia P, Rashid A, Fleming JB, Abdalla EK, Curley SA, Vauthey JN, Sood AK, Yao JC, Ellis LM. Identification of cancer stem cells in human gastrointestinal carcinoid and neuroendocrine tumors. Gastroenterology. 2011 Nov;141(5):1728-37.

40. Heverhagen AE, Geis C, Fendrich V, Ramaswamy A, Montalbano R, Di Fazio P, Bartsch DK, Ocker M, Quint K. Embryonic transcription factors CDX2 and Oct4 are overexpressed in neuroendocrine tumors of the ileum: A pilot study. Eur Surg Res. 2013;51(1-2):14-20.

41. Leithner K, Hrzenjak A, Trotzmuller M, Moustafa T, Kofeler HC, Wohlkoenig C, Stacher E, Lindenmann J, Harris AL, Olschewski A, Olschewski H. PCK2 activation mediates an adaptive response to glucose depletion in lung cancer. Oncogene. 2014 Mar 17

42. Pfaffl MW. A new mathematical model for relative quantification in real-time RT-PCR. Nucleic Acids Res. 2001 May 1;29(9):e45.

43. Brown M, Wittwer C. Flow cytometry: Principles and clinical applications in hematology. Clin Chem. 2000 Aug;46(8 Pt 2):1221-9.

44. Ribatti, D. The Chick Embryo Chorioallantoic Membrane in the Study of Angiogenesis and Metastasis. Netherlands: Springer; 2010. 119 p.

45. Deryugina EI, Quigley JP. Chapter 2. chick embryo chorioallantoic membrane models to quantify angiogenesis induced by inflammatory and tumor cells or purified effector molecules. Methods Enzymol. 2008;444:21-41.

46. Deryugina EI, Quigley JP. Chick embryo chorioallantoic membrane model systems to study and visualize human tumor cell metastasis. Histochem Cell Biol. 2008 Dec;130(6):1119-30.

47. Subauste MC, Kupriyanova TA, Conn EM, Ardi VC, Quigley JP, Deryugina EI. Evaluation of metastatic and angiogenic potentials of human colon carcinoma cells in chick embryo model systems. Clin Exp Metastasis. 2009;26(8):1033-47.

48. Dohle DS, Pasa SD, Gustmann S, Laub M, Wissler JH, Jennissen HP, Dunker N. Chick ex ovo culture and ex ovo CAM assay: How it really works. J Vis Exp. 2009 Nov 30;(33). pii: 1620. doi(33):10.3791/1620.

49. Rodda DJ, Chew JL, Lim LH, Loh YH, Wang B, Ng HH, Robson P. Transcriptional regulation of nanog by OCT4 and SOX2. J Biol Chem. 2005 Jul 1;280(26):24731-7.

50. Chen Y, Orlicky DJ, Matsumoto A, Singh S, Thompson DC, Vasiliou V. Aldehyde dehydrogenase 1B1 (ALDH1B1) is a potential biomarker for human colon cancer. Biochem Biophys Res Commun. 2011 Feb 11;405(2):173-9.

51. Alison MR, Guppy NJ, Lim SM, Nicholson LJ. Finding cancer stem cells: Are aldehyde dehydrogenases fit for purpose? J Pathol. 2010 Dec;222(4):335-44.

52. Li T, Su Y, Mei Y, Leng Q, Leng B, Liu Z, Stass SA, Jiang F. ALDH1A1 is a marker for malignant prostate stem cells and predictor of prostate cancer patients' outcome. Lab Invest. 2010 Feb;90(2):234-44.

53. Ma I, Allan AL. The role of human aldehyde dehydrogenase in normal and cancer stem cells. Stem Cell Rev. 2011 Jun;7(2):292-306.

54. Wang A, Chen L, Pu K, Zhu Y. Identification of stem-like cells in non-small cell lung cancer cells with specific peptides. Cancer Lett. 2014 Aug 28;351(1):100-7.

55. Luo L, Zeng J, Liang B, Zhao Z, Sun L, Cao D, Yang J, Shen K. Ovarian cancer cells with the CD117 phenotype are highly tumorigenic and are related to chemotherapy outcome. Exp Mol Pathol. 2011 10;91(2):596-602.

56. Chiou SH, Wang ML, Chou YT, Chen CJ, Hong CF, Hsieh WJ, Chang HT, Chen YS, Lin TW, Hsu HS, Wu CW. Coexpression of Oct4 and nanog enhances malignancy in lung adenocarcinoma by inducing cancer stem cell-like properties and epithelial-mesenchymal transdifferentiation. Cancer Res. 2010 Dec 15;70(24):10433-44.

57. Liu K, Lin B, Zhao M, Yang X, Chen M, Gao A, Liu F, Que J, Lan X. The multiple roles for Sox2 in stem cell maintenance and tumorigenesis. Cell Signal. 2013 5;25(5):1264-71.

58. O'Brien C, Kreso A, Ryan P, Hermans K, Gibson L, Wang Y, Tsatsanis A, Gallinger S, Dick J. ID1 and ID3 regulate the self-renewal capacity of Human colon cancer-initiating cells through p21. Cancer Cell. 2012 6/12;21(6):777-92.

59. Strojnik T, Røsland GV, Sakariassen PO, Kavalar R, Lah T. Neural stem cell markers, nestin and musashi proteins, in the progression of human glioma: Correlation of nestin with prognosis of patient survival. Surg Neurol. 2007 8;68(2):133-43.

60. Lukacs RU, Memarzadeh S, Wu H, Witte ON. Bmi-1 is a crucial regulator of prostate stem cell self-renewal and malignant transformation. Cell Stem Cell. 2010 Dec 3;7(6):682-93.

61. Tian T, Zhang Y, Wang S, Zhou J, Xu S. Sox2 enhances the tumorigenicity and chemoresistance of cancer stem-like cells derived from gastric cancer. Journal of Biomedical Research. 2012 9;26(5):336-45.

62. Kato Y, Kaneko MK. A cancer-specific monoclonal antibody recognizes the aberrantly glycosylated podoplanin. Sci Rep. 2014 Aug 1;4:5924.

63. Visvader J, Lindeman G. Cancer stem cells: Current status and evolving complexities. Cell Stem Cell. 2012 6/14;10(6):717-28.

64. Alison MR, Lim SM, Nicholson LJ. Cancer stem cells: Problems for therapy? J Pathol. 2011;223(2):148-62.

65. Cojoc M, Mäbert K, Muders MH, Dubrovska A. A role for cancer stem cells in therapy resistance: Cellular and molecular mechanisms. Semin Cancer Biol(0)

66. Jordan CT, Guzman ML, Noble M. Cancer stem cells. N Engl J Med. 2006 09/21; 2014/10;355(12):1253-61.

67. Mi JQ, Li JM, Shen ZX, Chen SJ, Chen Z. How to manage acute promyelocytic leukemia. Leukemia. 2012 Aug;26(8):1743-51.

68. Jackson B, Brocker C, Thompson DC, Black W, Vasiliou K, Nebert DW, Vasiliou V. Update on the aldehyde dehydrogenase gene (ALDH) superfamily. Hum Genomics. 2011 May;5(4):283-303.

69. Clay MR, Tabor M, Owen JH, Carey TE, Bradford CR, Wolf GT, Wicha MS, Prince ME. Single-marker identification of head and neck squamous cell carcinoma cancer stem cells with aldehyde dehydrogenase. Head Neck. 2010;32(9):1195-201.

70. Fujiwara D, Kato K, Nohara S, Iwanuma Y, Kajiyama Y. The usefulness of three-dimensional cell culture in induction of cancer stem cells from esophageal squamous cell carcinoma cell lines. Biochem Biophys Res Commun. 2013 5/17;434(4):773-8.

71. Rasheed ZA, Yang J, Wang Q, Kowalski J, Freed I, Murter C, Hong SM, Koorstra JB, Rajeshkumar NV, He X, Goggins M, Iacobuzio-Donahue C, Berman DM, Laheru D, Jimeno A, Hidalgo M, Maitra A, Matsui W. Prognostic significance of tumorigenic cells with mesenchymal features in pancreatic adenocarcinoma. J Natl Cancer Inst. 2010 Mar 3;102(5):340-51.

72. Jiang T, Collins BJ, Jin N, Watkins DN, Brock MV, Matsui W, Nelkin BD, Ball DW. Achaete-scute complex homologue 1 regulates tumor-initiating capacity in human small cell lung cancer. Cancer Res. 2009 Feb 1;69(3):845-54.

73. Michishita M, Akiyoshi R, Suemizu H, Nakagawa T, Sasaki N, Takemitsu H, Arai T, Takahashi K. Aldehyde dehydrogenase activity in cancer stem cells from canine mammary carcinoma cell lines. Vet J. 2012 Aug;193(2):508-13.

74. Prasmickaite, Lina , Engesæter, Birgit , Skrbo, Nirma , Hellenes, Tina , Kristian, Alexandr , Oliver, Nina K. , Suo, Zhenhe , Mælandsmo, Gunhild M. Aldehyde dehydrogenase (ALDH) activity does not select for cells with enhanced aggressive properties in malignant melanoma. PloS one. 2010;5:1-12.

75. Breitman TR, Selonick SE, Collins SJ. Induction of differentiation of the human promyelocytic leukemia cell line (HL-60) by retinoic acid. Proceedings of the National Academy of Sciences. 1980 May 01;77(5):2936-40.

76. Huang ME, Ye YC, Chen SR, Chai JR, Lu JX, Zhoa L, Gu LJ, Wang ZY. Use of all-trans retinoic acid in the treatment of acute promyelocytic leukemia. Blood. 1988 Aug;72(2):567-72.

77. Phillips TM, McBride WH, Pajonk F. The response of CD24-/low/CD44+ breast Cancer–Initiating cells to radiation. Journal of the National Cancer Institute. 2006 December 20;98(24):1777-85.

78. Wang R, Xu J, Juliette L, Castilleja A, Love J, Sung SY, Zhau HE, Goodwin TJ, Chung LW. Three-dimensional co-culture models to study prostate cancer growth, progression, and metastasis to bone. Semin Cancer Biol. 2005 Oct;15(5):353-64.

79. Chen H, Zhou L, Wan G, Dou T, Tian J. BMI1 promotes the progression of laryngeal squamous cell carcinoma. Oral Oncol. 2011 Jun;47(6):472-81.

80. Kim JH, Yoon SY, Jeong S, Kim SY, Moon SK, Joo JH, Lee Y, Choe IS, Kim JW. Overexpression of bmi-1 oncoprotein correlates with axillary lymph node metastases in invasive ductal breast cancer. The Breast. 2004 10;13(5):383-8.

81. Kim JH, Yoon SY, Kim C, Joo JH, Moon SK, Choe IS, Choe Y, Kim JW. The bmi-1 oncoprotein is overexpressed in human colorectal cancer and correlates with the reduced p16INK4a/p14ARF proteins. Cancer Lett. 2004 1;203(2):217-24.

82. Song W, Tao K, Li H, Jin C, Song Z, Li J, Shi H, Li X, Dang Z, Dou K. Bmi-1 is related to proliferation, survival and poor prognosis in pancreatic cancer. Cancer Science. 2010;101(7):1754-60.

83. Kawamoto M, Ishiwata T, Cho K, Uchida E, Korc M, Naito Z, Tajiri T. Nestin expression correlates with nerve and retroperitoneal tissue invasion in pancreatic cancer. Hum Pathol. 2007 2014/10;40(2):189-98.

84. Florenes VA, Holm R, Myklebost O, Lendahl U, Fodstad O. Expression of the neuroectodermal intermediate filament nestin in human melanomas. Cancer Res. 1994 Jan 15;54(2):354-6.

85. Wang X, Hu JF, Tan Y, Cui J, Wang G, Mrsny RJ, Li W. Cancer stem cell marker musashi-1 rs2522137 genotype is associated with an increased risk of lung cancer. PLoS One. 2014 May 2;9(5):e95915.

86. Potten CS, Booth C, Tudor GL, Booth D, Brady G, Hurley P, Ashton G, Clarke R, Sakakibara S, Okano H. Identification of a putative intestinal stem cell and early lineage marker; musashi-1. Differentiation. 2003 1;71(1):28-41.

87. Fan LF, Dong WG, Jiang CQ, Xia D, Liao F, Yu QF. Expression of putative stem cell genes musashi-1 and beta1-integrin in human colorectal adenomas and adenocarcinomas. Int J Colorectal Dis. 2010 Jan;25(1):17-23.

88. Shu HJ, Saito T, Watanabe H, Ito JI, Takeda H, Okano H, Kawata S. Expression of the Musashi1 gene encoding the RNA-binding protein in human hepatoma cell lines. Biochem Biophys Res Commun. 2002 Apr 26;293(1):150-4.

89. Han S, Guo C, Hong L, Liu J, ZheyiHan, Liu C, Wang J, Wu K, Ding J, Fan D. Expression and significance of Id1 helix–loop–helix protein overexpression in gastric cancer. Cancer Lett. 2004 12/8;216(1):63-71.

90. Meng Q, Jia Z, Wang W, Li B, Ma K, Zhou C. Inhibitor of DNA binding 1 (Id1) induces differentiation and proliferation of mouse embryonic carcinoma P19CL6 cells. Biochem Biophys Res Commun. 2011 8/26;412(2):253-9.

91. Takai N, Miyazaki T, Fujisawa K, Nasu K, Miyakawa I. Id1 expression is associated with histological grade and invasive behavior in endometrial carcinoma. Cancer Lett. 2001 Apr 26;165(2):185-93.

92. Cheng Y, Tsai J, Hsieh K, Yang Y, Chen Y, Huang M, Yuan S. Id1 promotes lung cancer cell proliferation and tumor growth through akt-related pathway. Cancer Lett. 2011 8/28;307(2):191-9.

93. Murase R, Sumida T, Liu Sh, Yoshimura T, Ishikawa A, Wei FC, Tano T, Hamakawa H. The expression and roles of Id1 and Id2 in the aggressive phenotype of human oral squamous cell carcinoma cells. Journal of Oral and Maxillofacial Surgery, Medicine, and Pathology. 2013 1;25(1):12-7.

94. Rothschild SI, Kappeler A, Ratschiller D, Betticher DC, Tschan MP, Gugger M, Gautschi O. The stem cell gene “inhibitor of differentiation 1” (ID1) is frequently expressed in non-small cell lung cancer. Lung Cancer. 2011 3;71(3):306-11.

95. Kumar SM, Liu S, Lu H, Zhang H, Zhang PJ, Gimotty PA, Guerra M, Guo W, Xu X. Acquired cancer stem cell phenotypes through Oct4-mediated dedifferentiation. Oncogene. 2012 Nov 22;31(47):4898-911.

96. Berezovsky AD, Poisson LM, Cherba D, Webb CP, Transou AD, Lemke NW, Hong X, Hasselbach LA, Irtenkauf SM, Mikkelsen T, deCarvalho AC. Sox2 promotes malignancy in glioblastoma by regulating plasticity and astrocytic differentiation. Neoplasia. 2014 3;16(3):193,206.e25.

6. SUPPLEMENTS

Table 12 Overview of performed CAM experiments and their results/15.000 cells

Matrigel™	Incub. time	Spheriods			Single cells		
		non	streak	tumour	non	streak	tumour
+	3 days	-	-	4	-	1	6
	4 days	-	-	8	-	-	3
	5 days	-	-	4	-	-	3
	6 days	-	-	4	-	-	3
-	3 days	2	7	12	-	4	-
	4 days	-	-	3	1	2	1
	5 days	-	-	3	1	1	2
	6 days	1	1	7	4	-	-

Table 13 Additional CAM experiment. Xenografts of spheroid with different cell number after 3 days

Number of cells	Spheroide without Matrigel								
	9000			16500			24000		
	non	streak	tumour	non	streak	tumour	non	streak	tumour
	-	2	-	-	-	2	-	-	2

Table 14 Additional CAM experiment. Xenografts of singel cells with different cell number after 3 days

Number of cells	Single cells with Matrigel					
	30000			$1x10^6$		
	non	streak	tumour	non	streak	tumour
	-	1	4	1	1	11

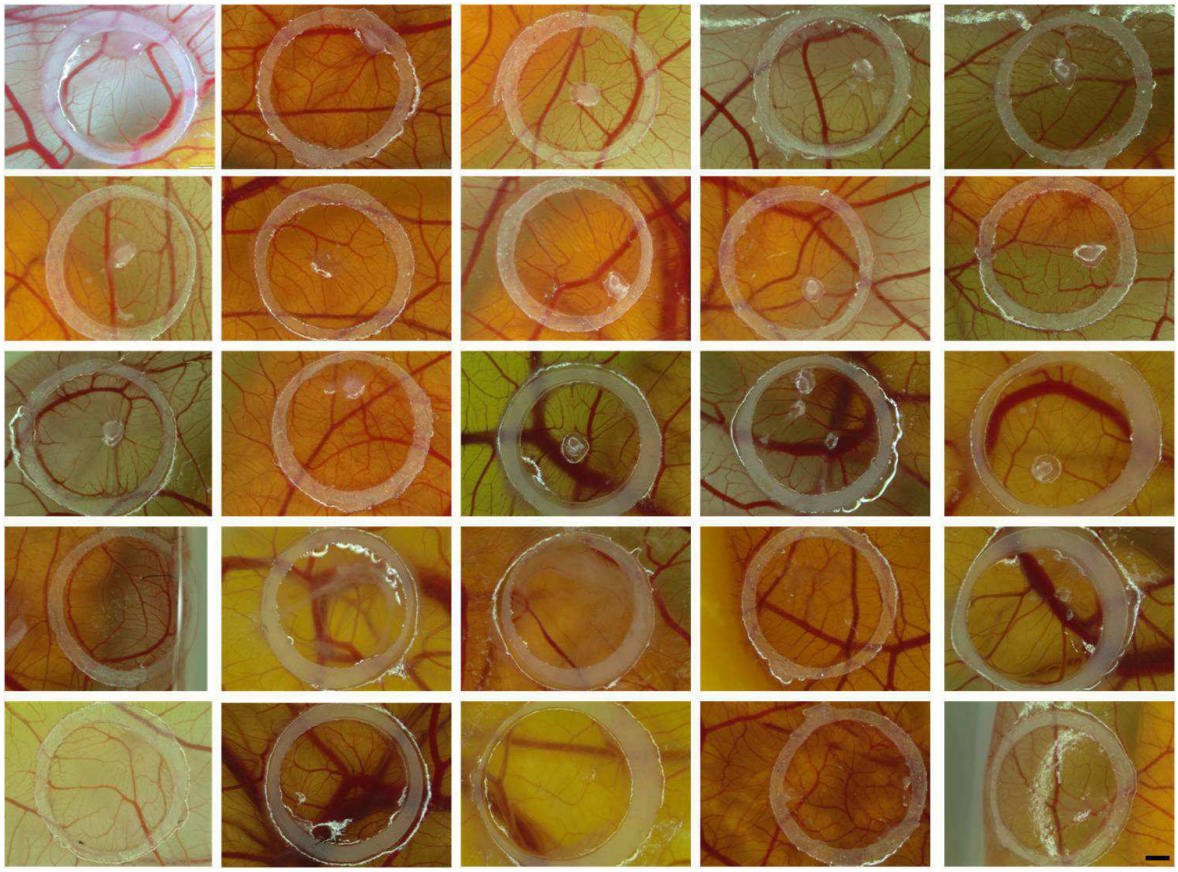

Figure 32 Overview of tumour formation of P-STS spheroids (15.000) xenografts after 3 days. Scale bar: 1mm

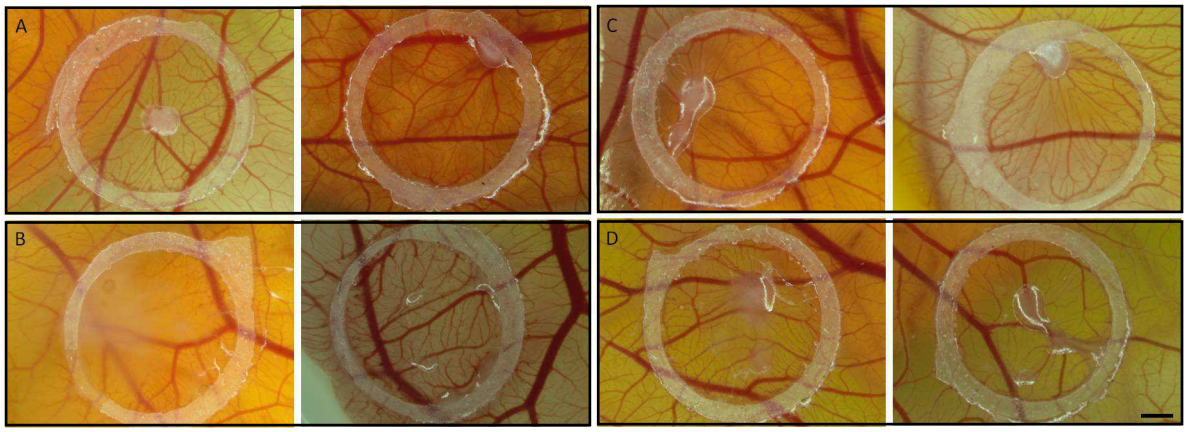

Figure 33 3 day incubated P-STS spheroide xenografts without matrigel, different cell number. A: 15000 cellen B:22500 cells C:30000 cells D37500 cells. Scale bar: 1mm

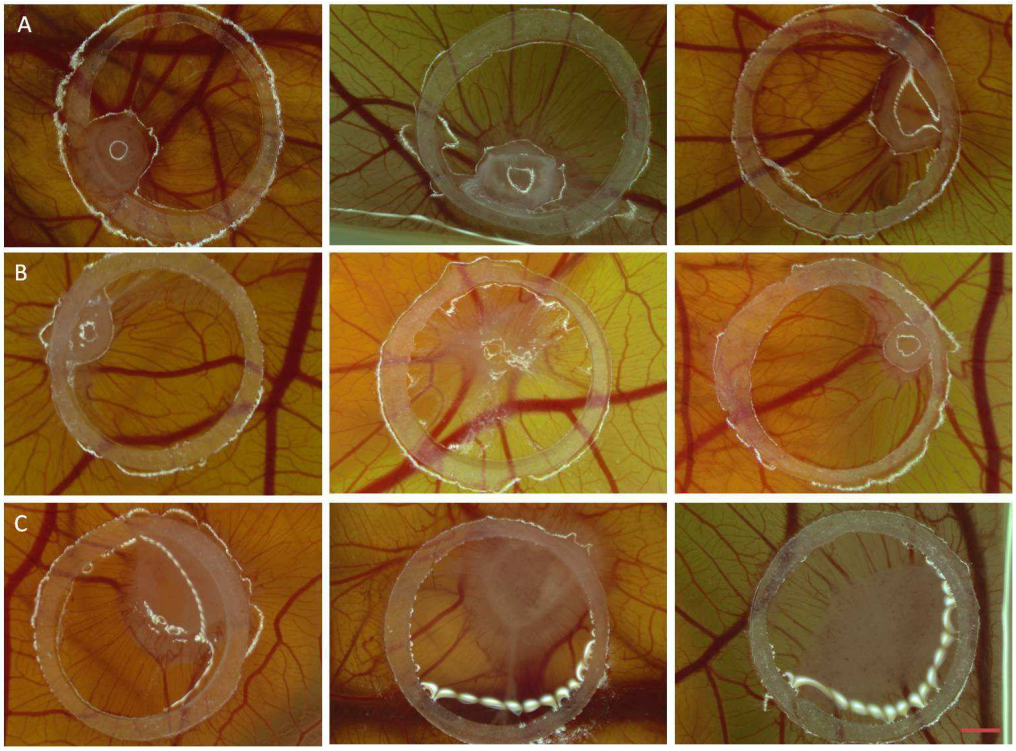

Figure 34 Tumour formation of P-STS single cell xenografts after 3 days with different cell numbers: A:15000, B:30000, C:1*10^6. Scale bar: 1mm

Detailed method manual

Cell culture - harvesting of P-STS cells

1. Mechanical dissociation of the cells with a scraper
2. Transfer the cell suspension in a 50 ml falcon tube
3. Centrifugation at 180 *g*
4. Remove old medium and resuspend the cell pellet with 3 ml fresh medium
5. Casy cell counting (10µl cell suspension in 10ml Casy solution)
6. Seed cells with $2x10^5$ cell/mL - total $1x10^6$ in 10mL

Spheroid formation - ultra low adhesion plates

1. Harvest cells explained above (1 - 5)
2. The total volume of each well is 200µl for the spheroid formation
   IMPORTANT: follow the correct order!
3. Calculate the volume you need to form spheroids with 7500 cell/well
   Example: $1x10^6$ cells/ml -> 7.5µl/well
4. Pipette 192.5µl medium in each well (200 µl -7.5 µl =192.5µl)
5. Take a 1.5 ml tube and pipette 720µl of the cell suspension in it
6. Fill up the wells with 7,5µl cell suspension from the 1.5 ml tube
7. Centrifuge the plate with 250 *g* for 10 minutes
8. Incubate the plate at 37°C and 5% CO_2
9. Spheroid formation control every day via microscope

FACS staining - CD 117

1. Harvest cells explained "Cell culture - harvesting of P-STS cells" (1 - 3)
2. Remove old medium and resuspend the cell pellet with 3 ml PBS
3. Casy cell counting (10µl cell suspension in 10ml Casy solution)
4. Prepare a FACS tube with $1x10^6$ cells in 100 µl
5. Add 2.5 µl antibody and mix the solution
6. 10 min incubation in the dark at 4°C
7. After incubation, centrifuge the FACS tube at 1300 rmp for 5 minutes
8. Wash the cell three times with 500µl PBS
9. Resuspend cells in 100µl PBS for the measurement

FACS staining - CD 24

1. Harvest cells explained "Cell culture - harvesting of P-STS cells" (1 - 3)
2. Remove old medium and resuspend the cell pellet with 3 ml PBS
3. Casy cell counting (10µl cell suspension in 10ml Casy solution)
4. Prepare a FACS tube with $1x10^6$ cells in 100 µl
5. Add 10 µl antibody and mix the solution
6. 10 min incubation in the dark at 4°C
7. After incubation, centrifuge the FACS tube at 180 *g* for 5 minutes
8. Wash the cell three times with 500µl PBS
9. Resuspend cells in 100µl PBS for the measurement

FACS staining - CD 133

1. Harvest cells explained "Cell culture - harvesting of P-STS cells" (1 - 3)
2. Remove old medium and resuspend the cell pellet with 3 ml PBS
3. Casy cell counting (10µl cell suspension in 10ml Casy solution)
4. Prepare a FACS tube with $1x10^6$ cells in 100 µl
5. Add 10 µl antibody and mix the solution
6. 10 min incubation in the dark at 4°C
7. After incubation, centrifuge the FACS tube at 180 *g* for 5 minutes
8. Wash the cell three times with 500µl PBS
9. Resuspend cells in 100µl PBS for the measurement

FACS staining - CD 24

1. Harvest cells explained "Cell culture - harvesting of P-STS cells" (1 - 3)
2. Remove old medium and resuspend the cell pellet with 3 ml PBS
3. Casy cell counting (10µl cell suspension in 10ml Casy solution)
4. Prepare a FACS tube with $1x10^6$ cells in 100 µl
5. Add 5 µl antibody and mix the solution
6. 10 min incubation in the dark at 4°C
7. After incubation, centrifuge the FACS tube at 180 *g* for 5 minutes
8. Wash the cell three times with 500µl PBS
9. Resuspend cells in 100µl PBS for the measurement

ALDH activity assay

1. Harvest cells explained "Cell culture - harvesting of P-STS cells" (1 - 3)
2. Remove old medium and resuspend the cell pellet with 3 ml PBS
3. Casy cell counting (10µl cell suspension in 10ml Casy solution)
4. Resuspend $1x10^6$ cells in 1000 µl ALDH assay buffer in a FACS tube with cab - test tube
5. Add 5µl DEAB in a second FACS tube (with cab) and name it "control"
6. Transfer 500µl of the test tube cell suspension in the control tube and mix it
7. 30 min incubation in the dark at 37°C
8. After incubation, centrifuge the FACS tube at 180 *g* for 5 minutes
9. Wash the cell three times with 500µl ALDH assay buffer
10. Resuspend cells in 500µl ALDH assay buffer for the measurement; up to the measurement store tubes on ice

Routine H+E for Paraffin Sections

1.	Xylene	2 changes, 2-3 minutes each (deparaffinizes sections)
2.	100% EtOH	2 changes, 2-3 minutes each (removes xylene)
3.	95% EtOH	2 changes, 2-3 minutes each
4.	70-80% EtOH	1 change, 2-3 minutes each
5.	Distilled H_2O	2-3 minutes (hydrates tissue)
6.	Hematoxylin (filtered)	1-5 minutes (stains nuclei) → 2 minutes with new Hematoxylin
7.	Rinse in H_2O	until excess stain is removed (water should remain clear, not blue colored
8.	0.5% acid alcohol	1-5 seconds (decolorizes background)
9.	Rinse in H_2O	Ammonia water 1-5 minutes (until sections appear blue)
10.	Rinse in H_2O	several changes – 3 minutes
11.	70-80% EtOH	2-3 minutes
12.	Eosin (filtered)	1-20 seconds, depending on how bright you want it **Dip in once and go out quickly!** (Be aware some tissues may be resistant to eosin staining because of age or fixative; in this case increase times to 1-5 minutes or more)

13.	95% EtOH	3 changes, 1 minute each (agitate slides in EtOH to remove excess eosin and to dehydrate evenly)
14.	100% EtOH	2 changes, 2-3 minutes each (dehydrate)
15.	Xylene	2 changes, 2-3 minutes each
16.	Mounting	e.g. Histomount and Coverslips

Protocol for Immunohistochemistry Staining

Deparaffinization:

1. 2x 10 min Xylol
2. 2x 5 min 100% EtOH
3. 2x 5 min 95% EtOH
4. 1x 5 min 70% EtOH
5. 30 sec. A. dest.

Antigen Retrieval (Unmasking of Antigens):

6. 7 min microwave (medium power) in Dako Retrieval pH 6.1 solution (dilute 10X to 1X with A. dest.)
7. Cool down 20 min
8. 2x 3 min in TBS
9. 30 sec. A. dest

Blocking:

10. Put slides in upright position, let them become touch dry and circle sections with DAKO-PEN
11. Add a sufficient amount of drops of Hydrogen Peroxide Block, incubate 10 min
12. 2x 3 min A. dest.
13. 15 min Protein Block (ca. 35 µl/section), DO NOT WASH!! Pat dry with tissue

Incubation with Antibodies:

14. 1° Antibody 1 h (RT) to overnight (4°C) – volume 35 µl/section, WET CHAMBER!!
15. 3x 3 min TBS
16. 10 min 2° Antibody Biotinylated Goat Anti-Polyvalent (mouse & rabbit) 35 µl, RT, WET CHAMBER!!
17. 3x 3 min TBS

Development and Detection:

18. 10 min Streptavidin Peroxidase, 35 µl, RT

19. 3x 3 min TBS
20. Incubate with Chromogen 1-10 min → mainly 4 min, observe under microscope & stop when ready
21. 2x 3 min A. dest.
22. 1 min with 1:10 diluted and freshly filtered Hematoxylin
23. 2x 2 min A. dest.
24. Dip 10x in Ammoniumwater/Scott's Water
25. 2x 2 min A. dest.
26. Cover with Aquatex and cover slip